

Supporting Information

Micro-Electro-Flow Reactor (μ -EFR) System for Ultra-Fast Arene Synthesis, and Manufacturing of Daclatasvir

Bhushan Mahajan,^{1,#} Taufiqueahmed Mujawar,¹ Subhash Ghosh, Srihari Pabbaraja,[#]
Ajay K. Singh[#]

Division of Organic Synthesis and Process Chemistry,
CSIR-Indian Institute of Chemical Technology, Hyderabad-500007, India.

[#] Academy of Scientific and Innovative Research (AcSIR), CSIR-Human Resource
Development Centre (CSIR-HRDC) Campus, Ghaziabad 201002, Uttar Pradesh, India
E-mail: srihari@iict.res.in; ajaysingh015@gmail.com;

[+] These authors contributed equally to this work.

Table of contents:

1.	General	S3
	1.1. Material and method used in experiments.	
	1.2. Measurement method.	
2.	General reaction procedure and fabrication of micro-electrolysis flow reactor (μ-EFR).	S4
	2.1. Micro-patterned nanoparticle deposited anode preparation.	
	2.1.1. <i>Ni@Cu anode preparation.</i>	
	2.1.2. <i>Pt@Ni@Cu anode preparation.</i>	
	2.2. Fabrication of μ -EFR.	
3.	3. General procedure for the synthesis of core biphenyl and DCV API:	S13
	3.1. Integrated continuous micro-flow platform for the synthesis, extraction and separation of core-biphenyl.	
	3.1.1. <i>Optimization of μ-EFR platform for synthesis of symmetrical arenes.</i>	
	3.1.2. <i>Optimization of micro-separator platform for extraction and separation of symmetrical arenes.</i>	
	3.1.3. <i>Procedure for synthesis, extraction and separation of symmetrical arenes.</i>	
	3.1.4. <i>Procedure for synthesis, extraction and separation of symmetrical arenes with unactivated para-substituted group.</i>	
4	Continuous flow DCV synthesis.	S25
	4.1. New generation continuous flow DCV synthesis.	
5.	Spectra	S37
6.	Supporting references	S66

1. General

1.1. Material and method used in experiments

Most of the reagents and chemicals are bought from Spectrochem, AVRA and Sigma-Aldrich, which were used as such without any further purification. Common organic chemicals and salts were purchased from AVRA chemicals, India. Water used was deionized water (18.2 mS conductivity) in the experiments. All work-up and purification procedures were carried out with reagent-grade solvents. Analytical thin-layer chromatography (TLC) was performed using analytical chromatography silica gel 60 F254 pre-coated plates (0.25 mm). The developed chromatogram was analysed by UV lamp (254 nm). PTFE (id = 100-1000 μm) tubing, T-junction and back-pressure controller (BPR) were procured from Upchurch IDEX HEALTH & SCIENCE. HPLC Pump used was from KNAUER. SS318 capillary bought from the spectrum market, Mumbai, India. Heating reactor used was from the Thales Nano Nanotechnology, Inc.

1.2. Measurement method.

Nuclear magnetic resonance (NMR) spectra were recorded on a Bruker 600, 500, 400 or 300 MHz in CDCl_3 or DMSO-d_6 solvent. Chemical shifts for ^1H NMR are expressed in parts per million (ppm) relative to tetramethylsilane (δ 0.00 ppm). Chemical shifts for ^{13}C NMR are expressed in ppm relative to CDCl_3 (δ 77.0 ppm). Data are reported as follows: chemical shift, multiplicity (s = singlet, d = doublet, dd = doublet of doublets, t = triplet, q = quartet, quin = quintet, sext = sextet, m = multiplet), coupling constant (Hz), and integration. For scanning electron microscopy (SEM), gold sputter coating was carried out on desired samples at pressure ranging in between 1 and 0.1 Pa. Sample was loaded in the chamber of JSM-7610F and recorded by operating at 10^{-2} to 10^{-3} Pa with EHT 15.00 kV with 300 V collector bias. LC-MS was conducted on Shimadzu technology LCMS-8040 instrument equipped with LUNA C8 ($250 \times 4.6\text{mm}$, 5.0 μm) and in

build triple quadrupole detector. GC/MS analysis was conducted on Shimadzu technology GCMS-QP2010 instrument equipped with a HP-5 column (30 m × 0.25 mm, Hewlett-Packard) and inbuilt MS 5975C VL MSD system with triple axis detector. Sonication (Power Sonic 405) was used for washing the metal surface. ATR analysis was conducted on Portable FTIR spectrometer Bruker ALPHA. High-resolution mass spectra (HRMS) were obtained from a JMS-T100TD instrument (DART) and Thermo Fisher Scientific Exactive (APCI). Datalog model DCS-PS-6401 power supply system was used to supply the constant current. Han's Yueming laser series (model CMA0604-B-A, Carbon dioxide based, laser power 60W) equipment was used for the fabrication of micro-channel.

2. General reaction procedure and fabrication of micro-electrolysis flow reactor (μ -EFR).

2.1. Micro-patterned nanoparticle deposited anode preparation:

Micro electro-flow outer body was fabricated with a stainless-steel body Fig. S1, (α : 60 mm length x 60 mm width x 10 mm thickness). The second layer was fabricated with teflon (60 mm length x 60 mm width x 1 mm thickness) layer made with laser cutter for protecting the stainless steel from the corrosive acid base and insulator for the current flow. Next, graphite cathode was customized as per the reactor size (60 mm length x 60 mm width x 2 mm thickness). For the solution flow under the constant current, third layer consisted of a laser cutted teflon plastic (60 mm x 60 mm x 1 mm thickness) zig-zag groove with rectangular shape (2 mm x 80.0 mm). Another copper electrode was customized as per the reactor size (60 mm length x 60 mm width x 2 mm thickness). After fabrication of each layer and to align the patterns, the 4-corners of each two teflon film were drilled to make a hole (1 mm diameter). Thereafter, both the electrodes were sandwiched by teflon zig-zag channel sheets with identical dimension to fit groove

channels and coupled to each other by inserting metal pins through the holes at the film corners (Fig. S1).

2.1.1. Ni@Cu anode preparation: Ni nanoparticles were patterned over copper plate made by electrodeposition method.^{S1} In this method, copper plate was cleaned by 2N acetic acid, followed by deionized water to remove oxidized layer and dried by N₂ flow. Then, the copper plate was sandwiched between the designed reactor and connected with pump (Fig. S1). Copper plate was connected with negative charge and graphite plate was connected with positive charge. Aqueous solution of Ni.acetate.H₂O (0.125 wt.%) was passed through the microreactor channel with flow rate of 100 $\mu\text{L min}^{-1}$ at 2V for 2 h, which typically led to the generation of an ash colored pattern, and then washed with water thoroughly to remove any unreacted salt and nanoparticle (Fig. S2 and S3).

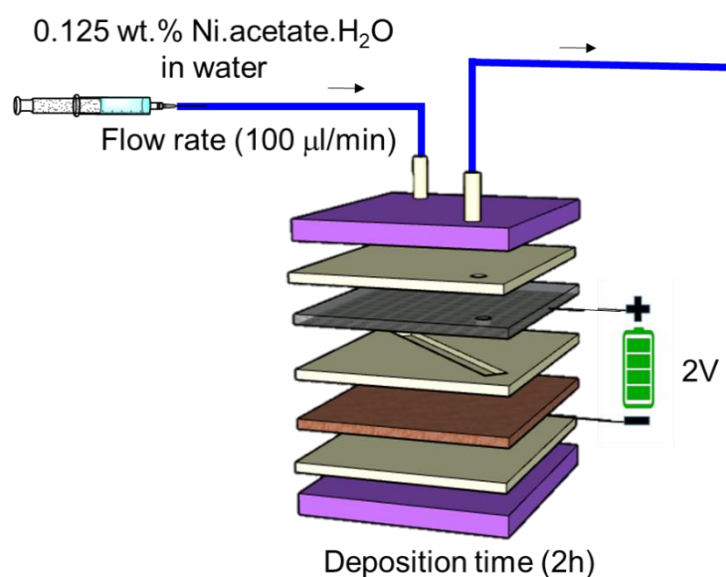


Fig. S1. Schematic diagram of continuous flow micro-patterned nickel nano-particle generation over the copper support.

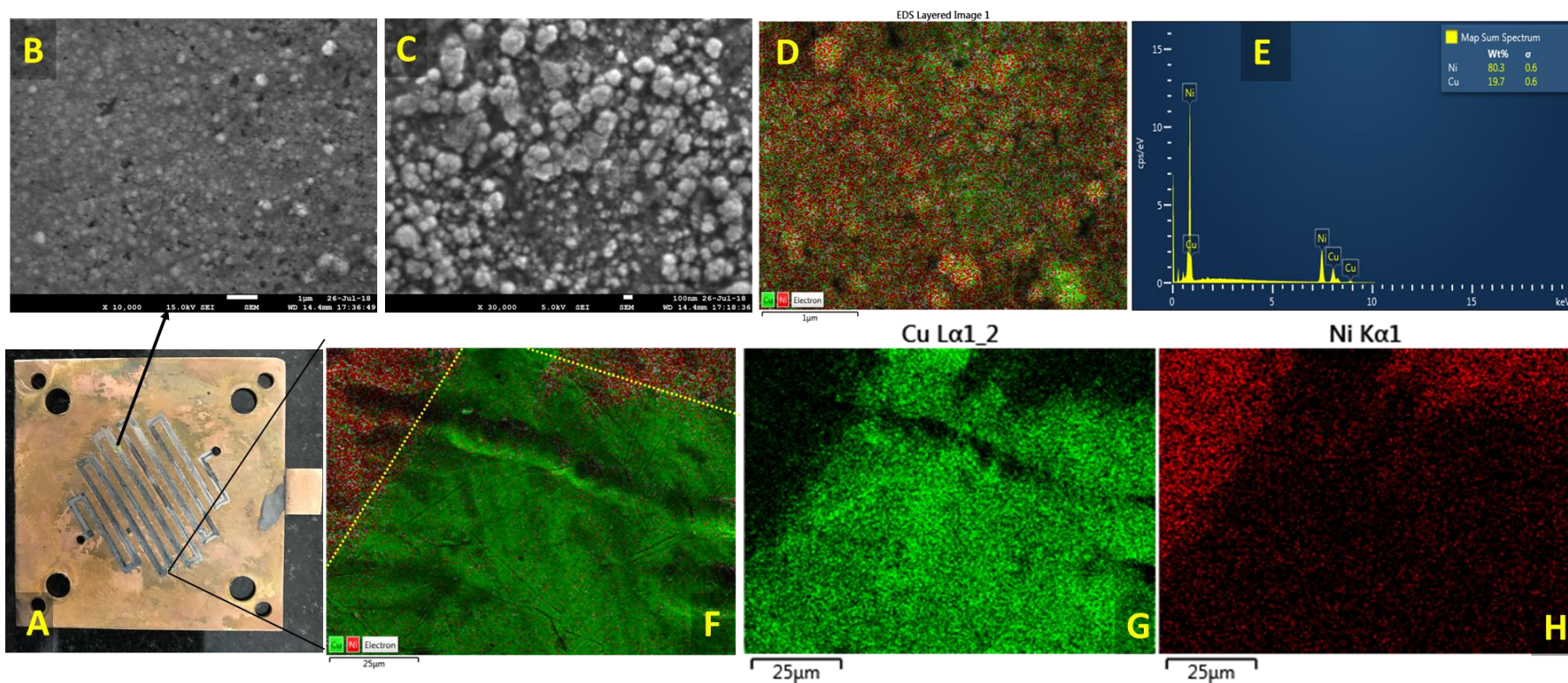


Fig. S2. Scanning Electron Microscopic, EDX and elemental mapping analysis of the Ni@Cu patterned electrode; (a) original image; (b) low resolution image; (c) high-resolution image; (d) high-resolution mix mapping of electrode; (e) EDX analysis data; (f) low resolution mix mapping at interface between Cu and Ni; (g) Cu elemental mapping; (h) Ni elemental mapping.

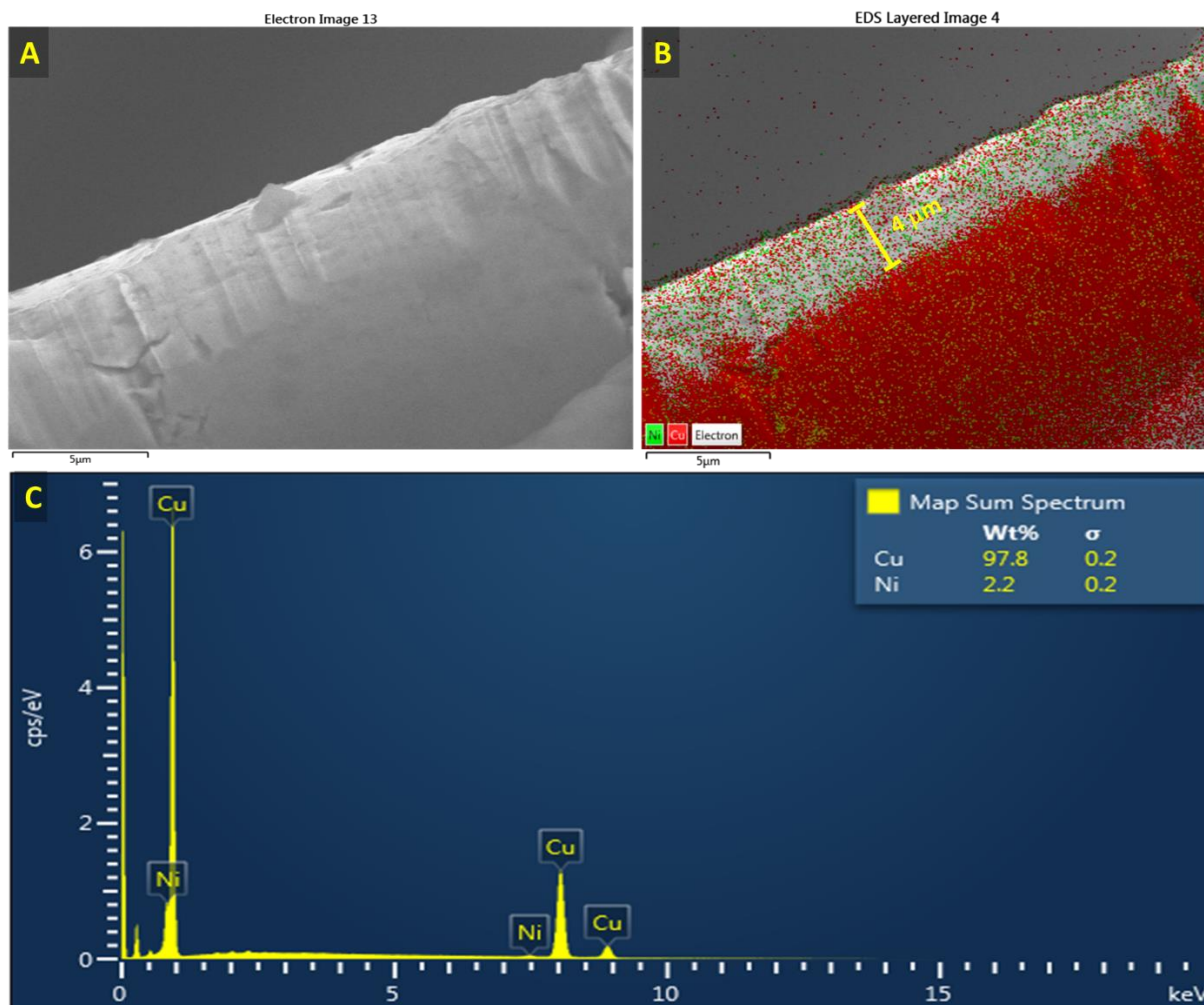


Fig. S3. EDX image of the Ni@Cu patterned electrode; (a) cross-section image; (b) mix mapping; (c) EDX analysis data.

2.1.2. Pt@Ni@Cu anode preparation: Modified phosphates bath-based method has been used for deposition of Pt over the Ni@Cu pre-deposited anode.² In this method, stock electrolytic solution containing mixture of Pt(IV) chlorides 150 mg, diammonium hydrogen phosphate $(\text{NH}_4)_2\text{HPO}_4$ 80 mg, disodium hydrogen phosphate $(\text{Na})_2\text{HPO}_4$ 200 mg, ammonium chloride 50 mg, and water 10 mL, was pumped with fix flow rate of $100 \mu\text{L min}^{-1}$ for 2h at 70°C under current density of 0.3 A/dm^2 , which typically led to the generation of a black colored patterning, and then washed with water thoroughly to remove any unreacted salt and nanoparticle (Fig. S5). Flower shape pattern morphology was confirmed by SEM/EDX (Fig.S5, S6).

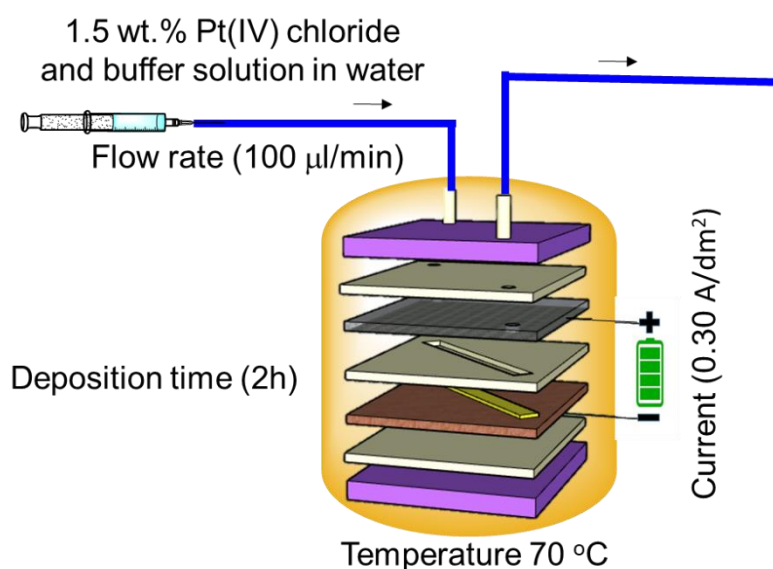


Fig. S4. Schematic diagram of continuous flow micro-patterned Pt nano-particle generation over the Ni@Cu anode.

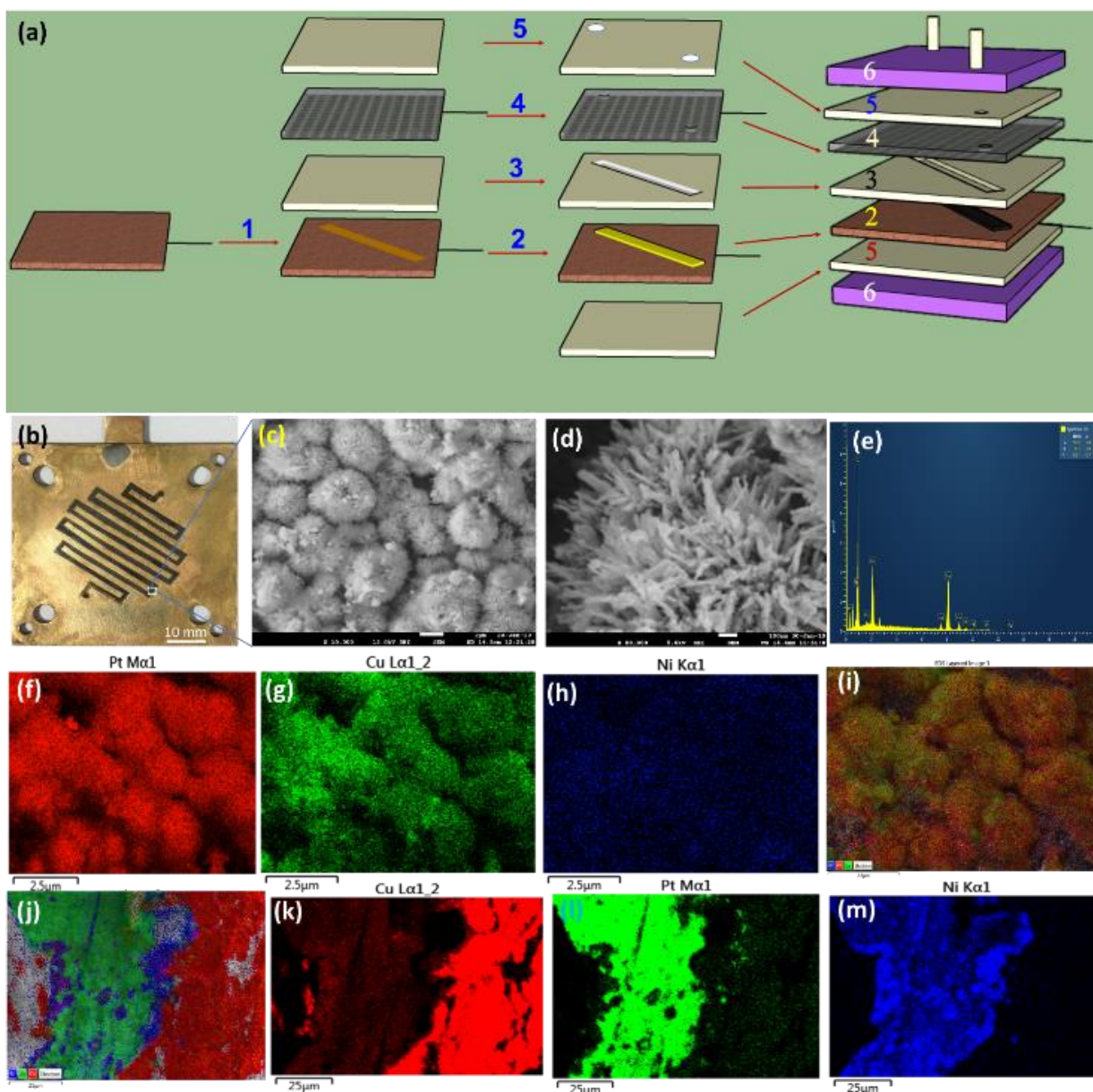


Fig. S5 Micro-electro flow reactor. (a) schematic illustration of fabrication of Micro-electro flow reactor; Step 1: patterning of Ni over the copper plate. Step 2: preparation of Pt nano-flower deposition over the Ni@Cu; Step 3: fabrication of laser grooved PFTE channel. Step 4: fabrication of graphite electrode; Step 5: fabrication of metal protection layer. Step 6: manual screw tight micro-electro flow reactor, showing one inlet and one outlets; (b) original image of the Pt@Ni@Cu micro-pattern electrode; (c&d) top view: low and high resolution SEM image respectively; (e) EDX graph from top view, (f-i) top view elemental Pt, Cu, Ni and mix mapping respectively; (j-h) cross-sectional mix mapping elemental, Pt, Cu, and Ni respectively.

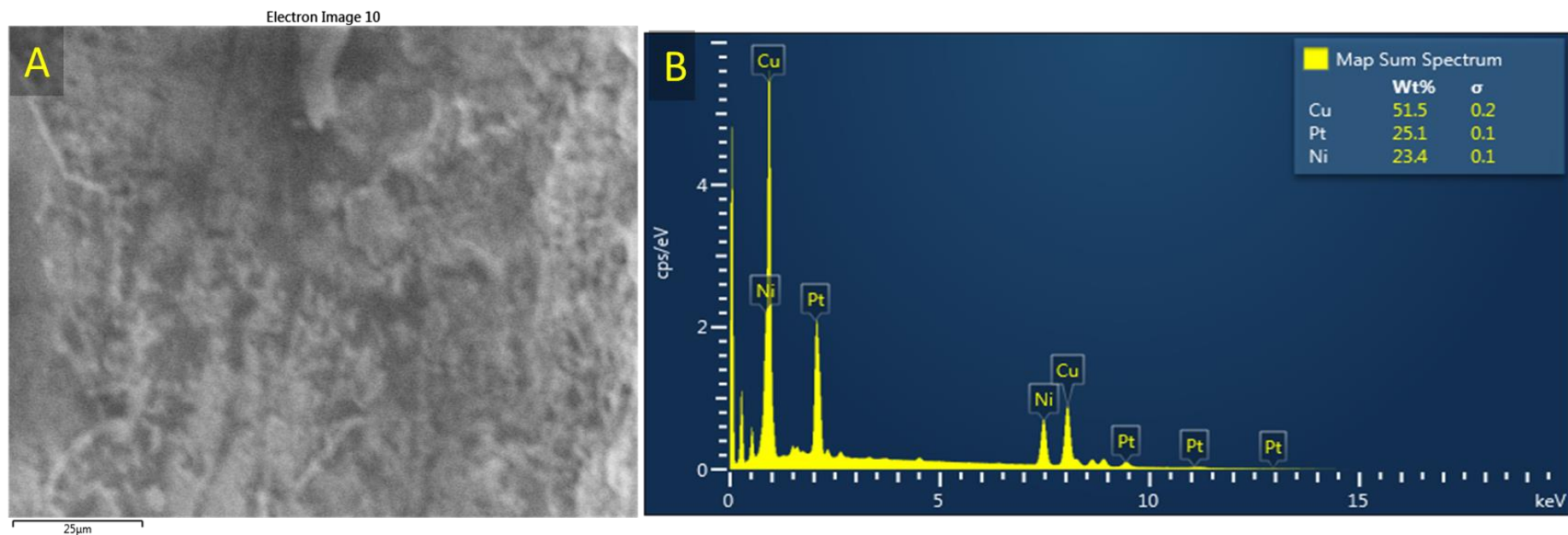


Fig. S6. (A) Cross-sectional SEM of Pt@Ni@Cu, (B) EDX of cross-sectional of Pt@Ni@Cu electrode.

2.2 Fabrication of μ -EFR: After the fabrication of nano-particle deposited electrode through electro-deposition method, the electrode was cleaned by washing with water under ultrasonic and dried. Polytetrafluoroethylene (PTFE) channel sandwiched by two electrodes with matching dimension of microchannel were placed between metal holder, the set was aligned by inserting metal pins through the holes at the film corners. Finally, the metal holder was tightly pressed by screw to seal the device with no leak (Fig.S7).

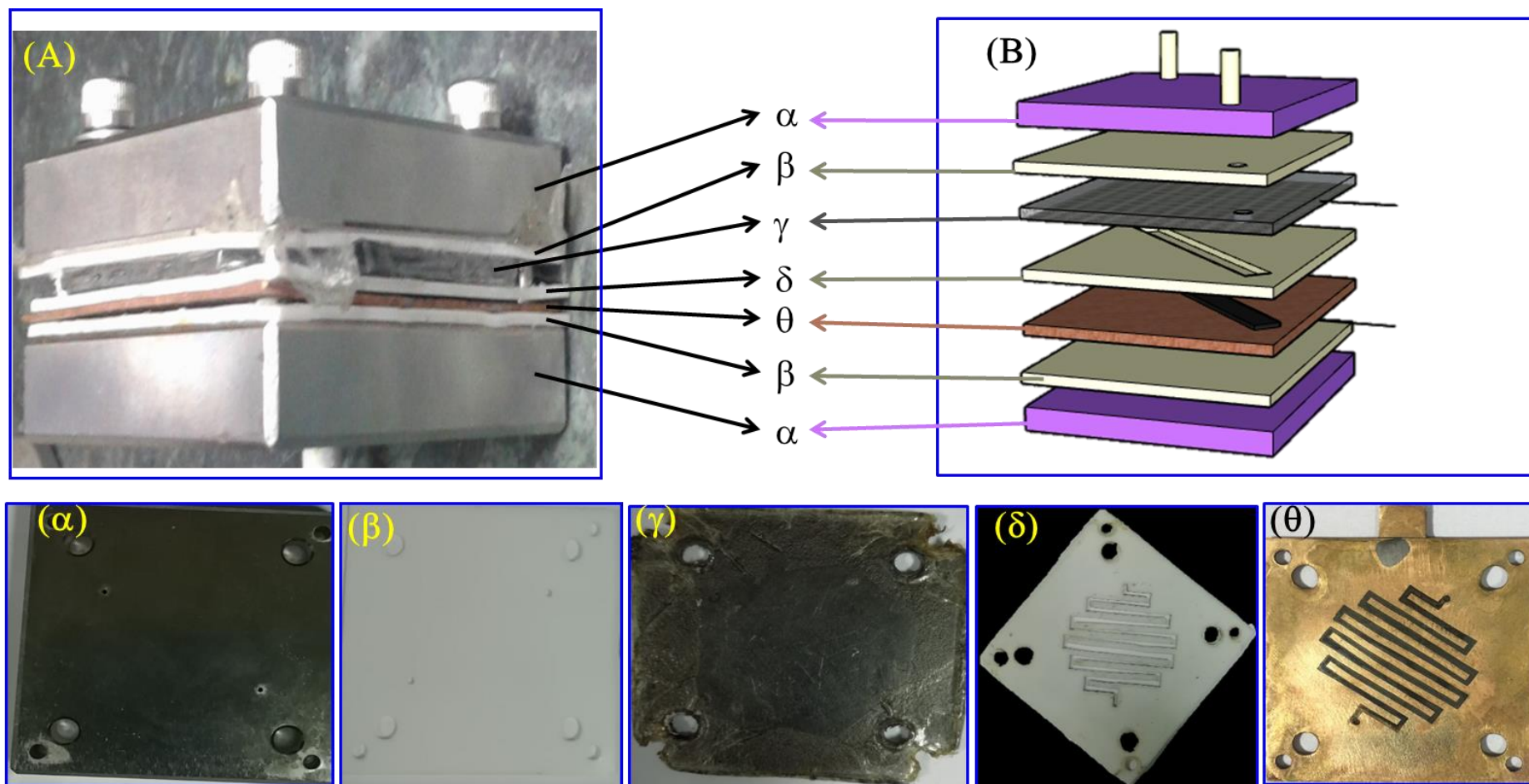


Fig. S7. Schematic presentation of micro-electro flow reactor; (A & B) original image and 3D model; (A) customized metal plate; (B) laser cut PTFE film; (C) customized graphite electrode; (D) Laser cut zig-zag PTFE channel; (E) Pt@Ni patterned structure.

3. General procedure for the synthesis of core biphenyl and DCV API:

3.1. Integrated continuous micro-flow platform for the synthesis, extraction and separation of core-biphenyl.

3.1.1. Optimization of μ -EFR platform for synthesis of symmetrical biphenyl:

We proceeded further by monitoring the model C-C coupling reaction of a solution containing bromobenzene(1a)/ NiCl₂.glyme/ bipyridine/ LiCl/ DMA, which was taken in the syringe and connected with above designed μ -EFR as described in (Fig. S8) to synthesize biphenyl. The solution, in a stoichiometric molar ratio of 10 (1a/ NiCl₂.glyme), was passed through a μ -EFR (reactor volume 200 μ L) containing Ni@Cu anode and graphite cathode held at 25 °C with current 4 mA at a flow rate of 50 μ L min⁻¹ (residence time = 4 min), which typically led to the generation of a brownish coloured solutions with 5% yield of the desired product **2a** (Table S1, entry 1). The use of various electrode combination of Ni/C, Ni foam/C, Cu/C, Pt/C, C/C, and Pt@Ni@Cu furnished **2a** (0–98%) (Table S1, entries 2–6). Notably, only the Pt@Ni@Cu anode was found to be the best system suitable for the ultra-fast biphenyl generation reaction (Table S1, entry 6). Assured of the feasibility of the μ -EFR with Pt@Ni@Cu anode system for use in C-C coupling reaction, we next examined the solvent effect. The use of either dimethylacetamide (DMA) or dimethylformamide (DMF) as a solvent led to complete conversion and excellent selectivity within 4 min, whereas tetrahydrofuran (THF), dimethylsulphoxide (DMSO), acetonitrile (MeCN), and water were not successful to produce the product in desired yield. Ligand screening experiments shows that the inexpensive combination of NiCl₂.glyme and a bipyridyl ligand (L₁) provides the most effective catalyst system for the transformation on bromobenzene (Table S1, entries 12-19). Optimized micro-electrolysis reaction conditions, 98% yield of **2a** was obtained in 4.0 min of residence time at

4 mA constant current, resulting in ca. 0.22 mmol h⁻¹ (0.82 g/day) productivity (Table S1, entry 6), while 4-7 h residence time was needed in batch electrolysis reaction under similar reaction condition. It was also observed that there was no electrode (Pt@Ni) degradation or leaching even after continuous running of experiments for 4 days.

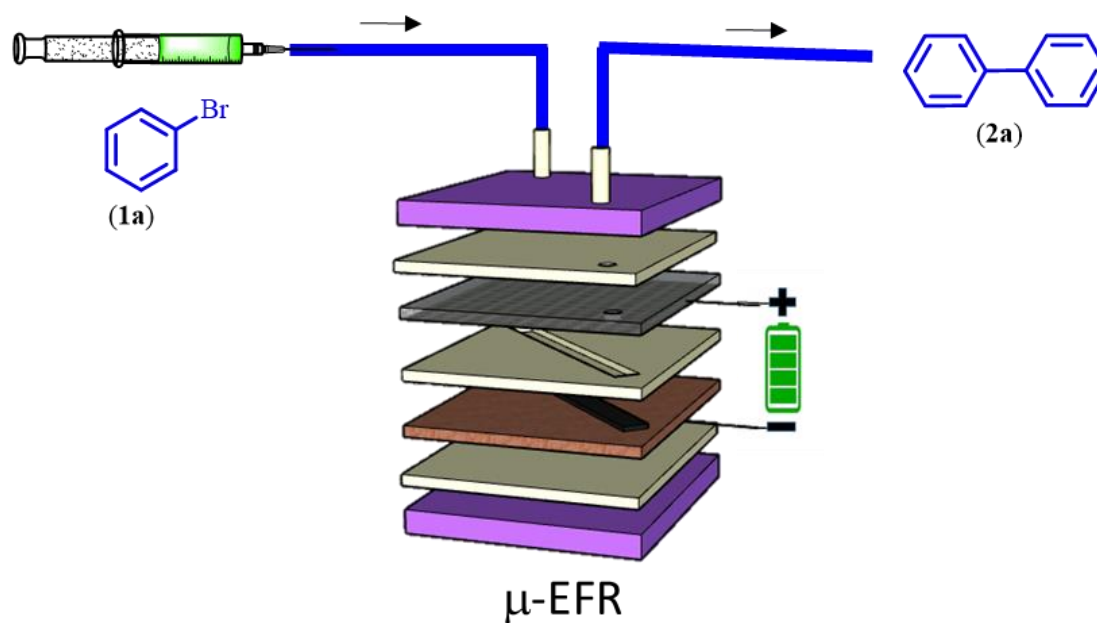
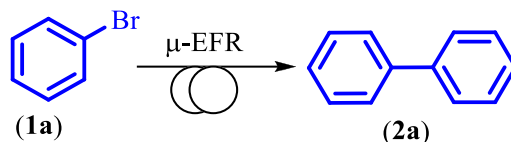


Fig. S8. Basic set up for the symmetrical arylation reaction.

Table S1. Evaluation of reaction optimization experiment with μ -EFR.



Conditions	Entry	Deviation from above	% Yield ^e
Effect of Anode (-) ^(a)	1	Ni/C	05
	2	Ni Foam/C	0
	3	Cu/C	0
	4	Pt/C	Trace
	5	C/C	0
	6	Pt@Ni@Cu/C	98
Effect of solvent ^(b)	7	DMF	87
	8	MeCN	5
	9	THF	Trace
	10	DMSO	34
	11	DMA/H ₂ O (9:1)	Trace
Effect of ligand ^(c)	12	L2	20
	13	L3	Trace
	14	L4	60
	15	L5	Trace
	19	NA	No reaction
Retention time (min.) ^(d)	17	1	73
	18	2	77
	19	10	98
	20	0.5	25

Reaction condition: bromobenzene (0.15 mmol), NiCl₂.glyme (10 mol%), bipyridine (L₁, 10 mol%), LiCl (4 eq.), DMA 0.01 M, current (4 mA), flow rate 50 μ L/min; **(a)** various anode; **(b)** anode (Pt@Ni@Cu); **(c)** bipyridine replace with difference ligand (10 mol%), anode (Pt@Ni@Cu), **(d)** anode (Pt@Ni@Cu), reaction time variation; **(e)** yield is based on GC-Mass analysis with anisole as internal standard.

3.1.2. Optimization of micro-separator platform for extraction and separation of symmetrical arenes.

Fabrication of microseparator: As shown in (Fig. S9), laser ablation on PTFE film was employed to fabricate the proposed dual channel device. The PTFE film layers of 1000 μm thick were ablated by UV laser 355 nm, to form serpentine microchannel (1000 μm width, 1000 μm depth and 80 cm length) as per our previously reported procedure.³ The 4-corners of each film were drilled to make holes of 1 mm diameter to align the film patterns. After laser ablation, the films were cleaned by washing with DCM under ultrasonic and dried. Polypropylene coated polytetrafluoroethylene (PTFE) membrane (Whatmann, 0.45 μm pore, 47 mm dia.) was sandwiched by two sheets of PTFE film with microchannel. The sandwich was in turn covered by metal protecting PTFE films and covered by metal holder. All the sheets were aligned by inserting metal pins through the holes at the film corners (Fig. S9). Finally, the metal holder was tightly pressed by screw to seal the device with no leak.

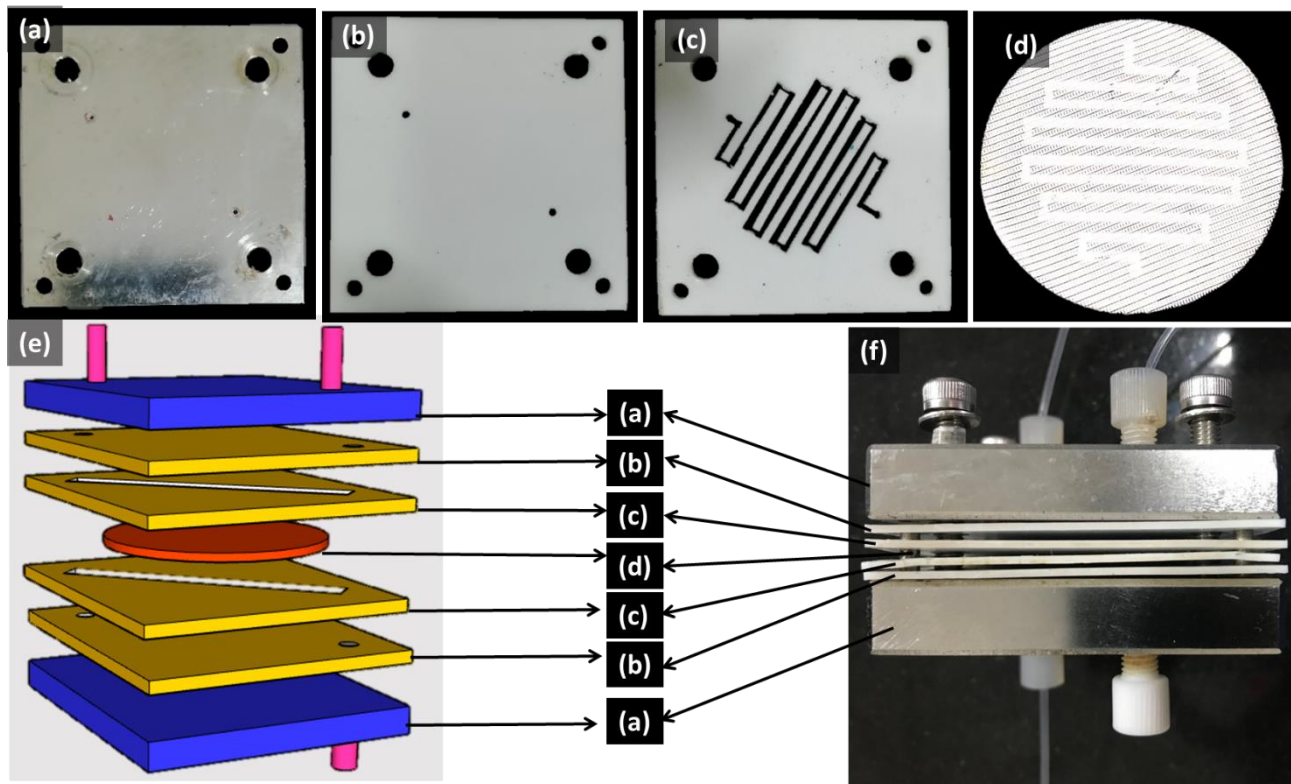
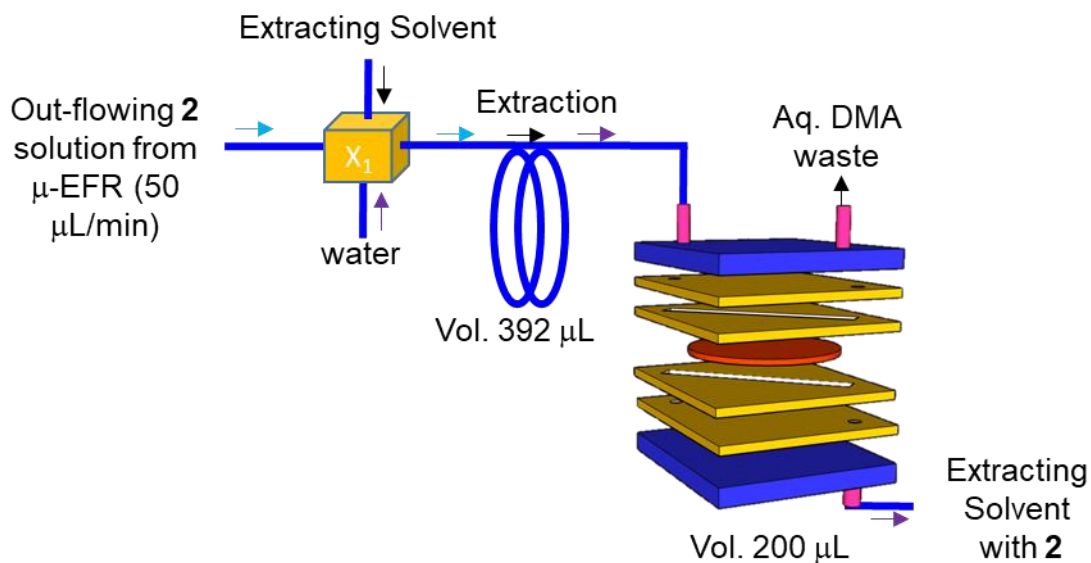


Fig. S9. Illustration of a fluoropolymer PTFE membrane based microseparator; (a) SS-metal body; (b) metal protecting PTFE layer; (c) laser grooved PTFE channel; (d) propylene coated PTFE membrane. (e) 3D model; (f) original photograph.

Solvent exchange optimization: To switch the solvent containing product from DMA to low volatile solvent DCM, the additional PTFE membrane embedded phase separator was connected to the outlet of the μ -EFR reactor as shown in (Table S2). A serial process of droplet formation, extraction and separation for purification of the symmetrical biaryls was conducted in droplet microfluidics equipped with the PTFE membrane microseparator, as explained in a stepwise manner. Step 1: At first, formation of alternating organic-aqueous droplets by introducing water into the product mixture in DMA through X-junction. Secondly, extraction of reaction wastes into aqueous stream by passing through a length of 0.5 m capillary during 0.7 min. Step 2: Finally, complete separation of the mixture of reactant, catalyst and product containing organic phase by wetting and crossing through thin fluoropolymer membrane to the bottom of the separator, whereas the waste aq. DMA containing aqueous phase did not wet the membrane and passed as the original stream (Table S2).

Table S2. Solvent exchange through the micro-separator.

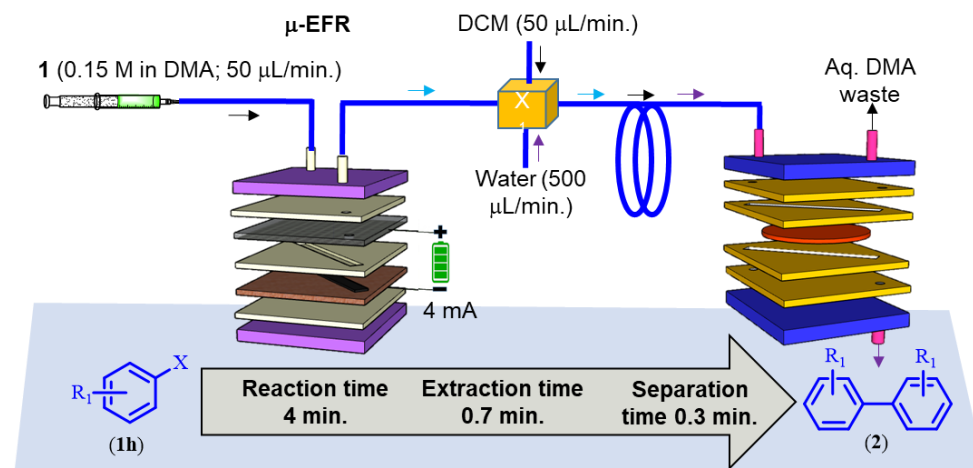


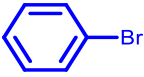
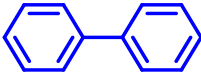
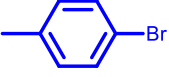
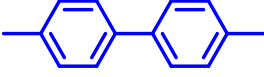
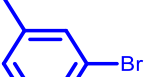
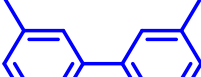
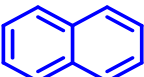
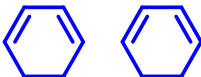
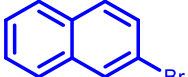
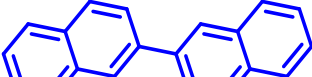

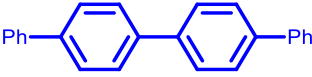
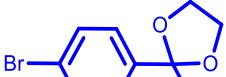
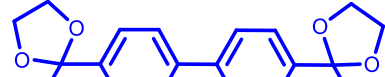
Entry	Flow rate (μL/min.)		Extraction time (min.)	Separation time (min.)	Extracting solvent	% Yield 2a
	Solvent	Water				
1	50	500	0.65	0.33	DCM	98
2	20	500	0.68	0.35	DCM	97
3	100	500	0.65	0.33	DCM	95
4	100	100	2.2	1.2	DCM	41
5	50	500	0.65	0.33	Toluene	94
6	50	500	0.65	0.33	DEE	98
7	50	500	0.65	0.33	MTBP	98

Yields are based on GC-MS analysis using anisole as an internal standard; average of two measurements.

3.1.3. Procedure for the synthesis, extraction and separation of symmetrical arenes.

Table S3: Comparative table of macro and integrated continuous micro-flow electrolysis reaction for the C-C coupling reaction.

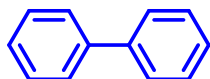


Entry	Substrate (1)	Product (2)	[% yield in our study]/ (Comparative result) ^{ref.}
1	 1a	 2a	[98]/ (Pd, 100 %, 100 °C, K ₂ CO ₃ base, 24 h; ⁴ Pd/C, Zn, CO ₂ , 91%, 15 hr) ⁵
2	 1b	 2b	[91]
3	 1c	 2c	[90]
4	 1d	 2d	[74]/ (Pd-PEOOSI-IPr, t-BuLi, 92%, 10 min) ⁶
5	 1e	 2e	[65]/(Pd-PEOOSI IPr, 62%, 1h) ⁷
6	 1f	 2f	[72]
7	 1g	 2g	[89]

The stock solution containing a mixture of bromobenzene (**1a**) (15 mmol) and NiCl₂.glyme (10 mol%), 2,2'-bipyridine (10 mol%), LiCl (6 mmol) in 100 mL of DMA was passed through the pre-designed μ -EFR, keeping 4 min. residence time and 4 mA constant current. The reaction mixture was quenched, and solvent exchange was achieved (from high boiling solvent DMA to low boiling solvent DCM by introducing water and low boiling solvent (DCM) through additional X-mixer to form organic-aqueous droplets (Table S3). Complete extraction between the organic-aqueous segments was observed with 0.7 min retention time by flowing through a PTFE capillary (id = 1000 μ m, length = 0.5 m, vol. = 392 μ L). Further, organic-aqueous segment was separated by passing through the above designed homemade microseparator and complete separation was achieved by regulating the back pressure with a retention time (0.3 min), flow rate of water (500 μ L/min) and flow rate of DCM (50 μ L/min). The extracted waste aqueous layer was further extracted with DCM and analyzed by GC-MS, which showed no product and was also confirmed by the absence of the corresponding peaks in the crude NMR analysis (¹H and ¹³C NMR spectra). Under similar extracting conditions, several other solvents were tested even for the replacement of DCM with diethyl ether, toluene, MTBP solvent and could see that the results are encouraged. The extracting solvent was removed under reduced pressure and the residue was purified by column chromatography (hexane/ethyl acetate) to give the product **2a-2g**.

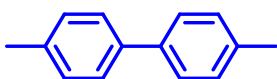
Note: Distribution ratio is very important parameter for the liquid-liquid membrane based extraction of the product. In optimized solvent distribution ratio, we need to use 1:10:1 ratio of DMA: Water: DCM.

Biphenyl (**2a**):



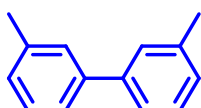
The title compound of (**2a**) was prepared according to the general procedure as described in section 3.2. The extracted mixture was purified by silica gel column chromatography (100% petroleum ether) to provide an off-white solid (**2a**), melting point: 69 °C. The spectra data matched with values reported in the literature. ⁸ ¹H NMR (500 MHz, CDCl₃) δ 7.70 – 7.65 (m, 4H), 7.54 – 7.49 (m, 4H), 7.45 – 7.39 (m, 2H). ¹³C NMR (126 MHz, CDCl₃) δ 141.20, 128.72, 127.21, 127.12. IR (ν_{max}): 3046, 1479, 1429, 739, 698 cm⁻¹; MS (EI): found: *m/z* 154 (M⁺).

4, 4'-dimethyl-1,1'-biphenyl (**2b**):



The title compound of (**2b**) was synthesised following the procedure described section 3.2 and general procedure involving **1b** as the corresponding substrate. The crude material was purified by silica gel column chromatography (100% PE) to provide a white solid (**2b**); melting point: 118 °C; The spectra data matched with values reported in the literature. ⁹ ¹H NMR (400 MHz, CDCl₃) δ 7.47 (d, *J*=7.9, 4H), 7.22 (d, *J*=7.8, 4H), 2.38 (s, 6H). ¹³C NMR (101 MHz, CDCl₃) δ 138.26, 136.66, 129.41, 126.78, 21.06. IR (ν_{max}): 3020, 2924, 2856, 1495, 1106, 1026, 801, 706 cm⁻¹; MS (EI): found: *m/z* 182 (M⁺).

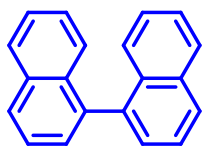
3, 3'-dimethyl-1, 1'-biphenyl (**2c**):



The title compound of (**2c**) was synthesised following the procedure described section 3.2 and general procedure involving the substrate **1c**. The crude material was purified by silica gel column chromatography (100% PE) to provide a white solid (**2c**) (0.17 mmol/h, 76%); Melting point: 150 °C; The spectra data matched with values reported in the literature. ¹⁰ ¹H NMR (400 MHz, CDCl₃) δ 7.40 – 7.28 (m, 4H), 7.23 (t, *J* = 7.5 Hz, 2H), 7.06 (d, *J* = 7.3 Hz, 2H), 2.33 (s, 6H). ¹³C NMR (101 MHz, CDCl₃) δ 141.33, 138.21, 128.57, 127.95, 127.88, 124.26, 21.52. IR (ν_{max}):

3021, 2924, 1600, 1472, 1216, 758, 708, 66. cm^{-1} ; MS (EI): found: m/z 182 (M^+).

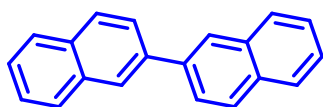
1,1'-binaphthalene (**2d**):



The title compound of (**2d**) was synthesised following the procedure described section 3.2 and general procedure involving substrate (**1d**).

The crude material was purified by silica gel column chromatography (100% PE) to provide a white solid (**2d**); Melting point: 159 °C. The spectra data matched with values reported in the literature. 7 ^1H NMR (500 MHz, CDCl_3) δ 7.92 (dd, J = 26.7, 5.5 Hz, 4H), 7.66 – 7.55 (m, 2H), 7.54 – 7.43 (m, 4H), 7.40 (t, J = 12.7 Hz, 2H), 7.27 (t, J = 7.0 Hz, 2H). ^{13}C NMR (101 MHz, CDCl_3) δ 138.42, 133.49, 132.82, 128.12, 127.86, 127.80, 126.53, 125.94, 125.77, 125.35. IR (ν_{max}): 3023, 1215, 740, 670 cm^{-1} ; MS (EI): found: m/z 254.11 (M^+).

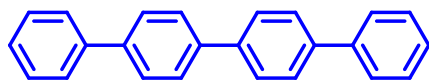
2, 2'-binaphthalene (**2e**):



The title Compound of (**2e**) was synthesised following the procedure described section 3.2 and general procedure

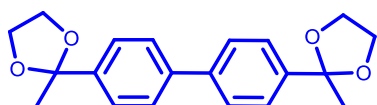
involving substrate (**1e**). The crude material was purified by silica gel column chromatography 100% PE) to provide a white solid (**2e**) (0.16 mmol/h, 73%); Melting point: 184 °C; the spectra data matched with values reported in the literature. 7 ^1H NMR (400 MHz, CDCl_3) δ 7.94 (d, J = 4.3 Hz, 4H), 7.58 (t, J = 7.4 Hz, 2H), 7.55 – 7.44 (m, 4H), 7.39 (d, J = 8.1 Hz, 2H), 7.26 (dd, J = 18.2, 11.1 Hz, 2H). ^{13}C NMR (126 MHz, CDCl_3) δ 138.43, 133.49, 132.82, 128.12, 127.86, 127.80, 126.53, 125.95, 125.78, 125.35. IR (ν_{max}): 3023, 1215, 741, 670 cm^{-1} ; MS (EI): found: m/z 254.11 (M^+).

1, 1':4', 1'':4'', 1''':4'''-quaterphenyl (**2f**):



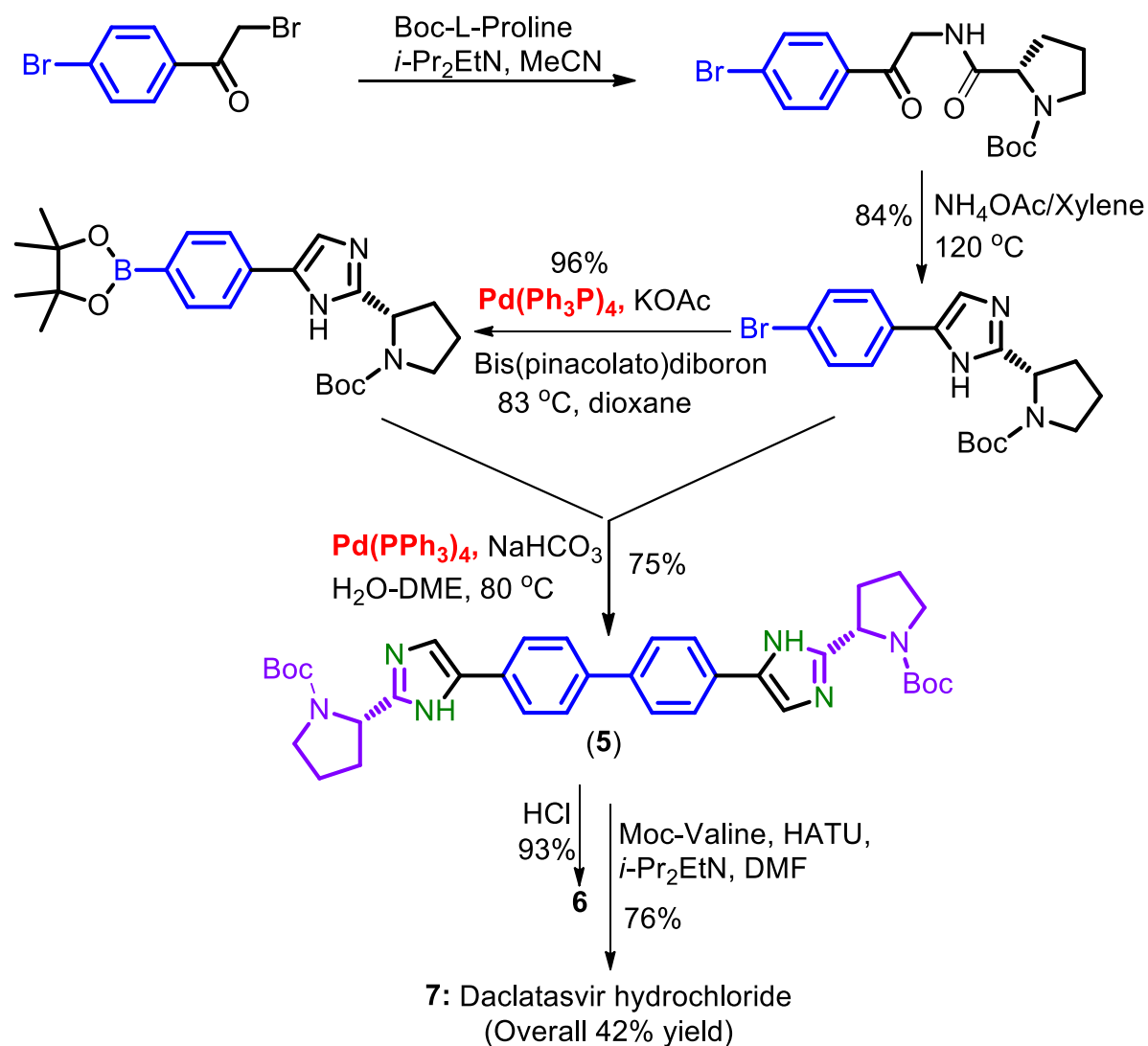
The title Compound of (**2f**) was synthesised following the procedure described in Section 4.1 with substrate (**1f**). The crude material was purified by silica gel column chromatography (100% PE) to provide a white solid (**2f**) (0.16 mmol/h, 72%); Melting point: 298 °C. The spectra data matched with values reported in the literature. ¹¹ ¹H NMR (500 MHz, CDCl₃) δ 7.61 – 7.55 (m, 8H), 7.47 – 7.43 (m, 8H), 7.38 (t, *J* = 7.3 Hz, 2H). ¹³C NMR (126 MHz, CDCl₃) δ 140.11, 139.97, 131.90, 128.86, 128.87, 127.68, 126.98, 121.57. IR (*v*_{max}): 3734, 3422, 3026, 2928, 1958, 1897, 1727, 1659, 1592, 1476, 1391, 1272, 1211, 1076, 1004, 828, 756, 693 cm⁻¹; MS (EI): *m/z* 306.14 (M⁺).

1, 1'-([1, 1'-biphenyl]-4,4'-diyl) diethanone (**2g**):

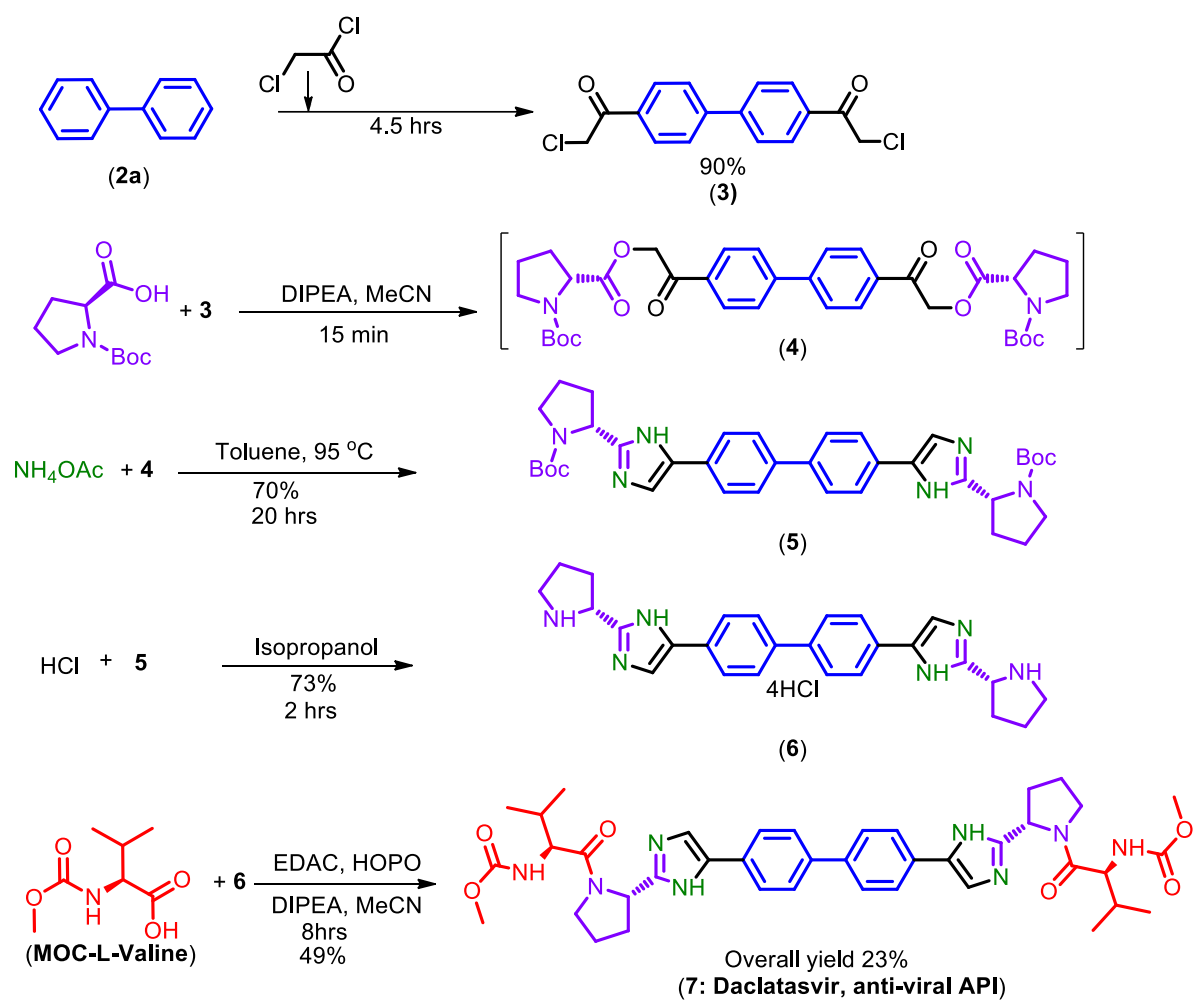


Compound (**2g**) was synthesised following the procedure described in Section 4.1 with substrate (**1g**). The crude material was purified by silica gel column chromatography (hexane/ethyl acetate; 95:05) to provide a white solid (**2g**); melting point: 148 °C; ¹H NMR (400 MHz, CDCl₃) δ 7.49 – 7.44 (m, 4H), 7.38 – 7.33 (m, 4H), 4.03 (td, *J* = 6.1, 4.2 Hz, 4H), 3.75 (td, *J* = 6.1, 4.2 Hz, 4H), 1.63 (s, 6H). ¹³C NMR (75 MHz, CDCl₃) δ 142.44, 131.28, 127.13, 121.83, 108.41, 64.45, 27.49. IR (*v*_{max}): 3390, 2980, 2888, 1479, 1383, 1245, 1197, 1082, 1031, 876, 825 cm⁻¹; MS (EI): *m/z* 326.15 (M⁺)

4: Continuous flow DCV synthesis:



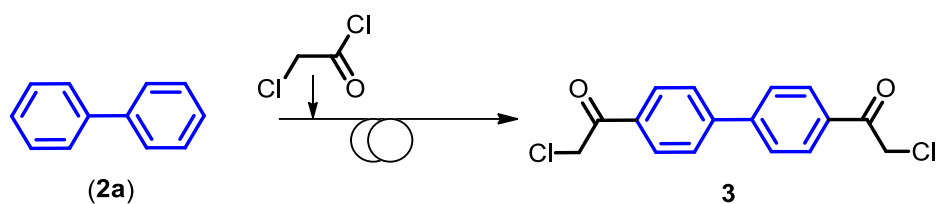
Scheme S1. First generation novel metal assisted DCV synthesis.¹²



Scheme S2. Second generation batch protocols for the synthesis of DCV.¹³

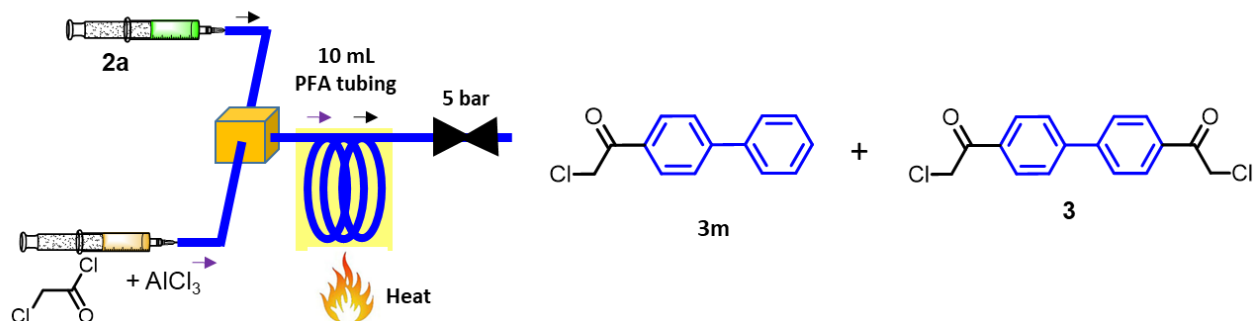
4.1. New generation continuous flow synthesis.

Step 1: Friedel-Craft acylation



A solution of compound **2a** in DCE was charged in one syringe. 2-Chloroacetyl chloride, various lewis acid (aluminum chloride, aluminum bromide, ferric chloride, tin chloride, or stannic chloride) dissolved in DCE was charged in the capillary microreactor with a T-mixer using separate syringe pumps (Fig.S10). The two solutions were introduced into a T-mixer in a varied flow rate and ratio to maintain the stoichiometry, and then passed through PTFE tubing for Friedel-Craft acylation reaction. Optimization conditions were varied depending on the nature of the catalyst reagent, retention time, temperature, and pressure etc (Table S4).

Table S4. Optimization of continuous micro-flow reaction to synthesize daclatasvir intermediate **3** ultra-fast manner.



Entry	Flow rate ($\mu\text{L}/\text{min}$)		Temperature ($^{\circ}\text{C}$)	Pressure (bar)	Retention time (min.)	Yield (%)	
	Compound 2a	2-chloro acetyl chloride				8m	8
1 ^a	100	100	40	1	50	36	10
2 ^a	100	100	40	5	50	44	20
3 ^a	100	100	80	5	50	*	*
4 ^b	100	200	80	5	33.3	12	7
5 ^b	100	250	80	5	28.6	0	98

Reaction condition: (a) **2a**: 0.25 M in DCM; mixture of chloroacetyl chloride and Aluminum chloride (0.625 M in DCM with 1:1 molar ratio); (b) **2a**: 0.16 M in DCE; mixture of chloroacetyl chloride and Aluminum chloride (0.4 M in DCE with 1:1 molar ratio); Yields are based on isolated yields; * represent the tube blocking problem was encountered.

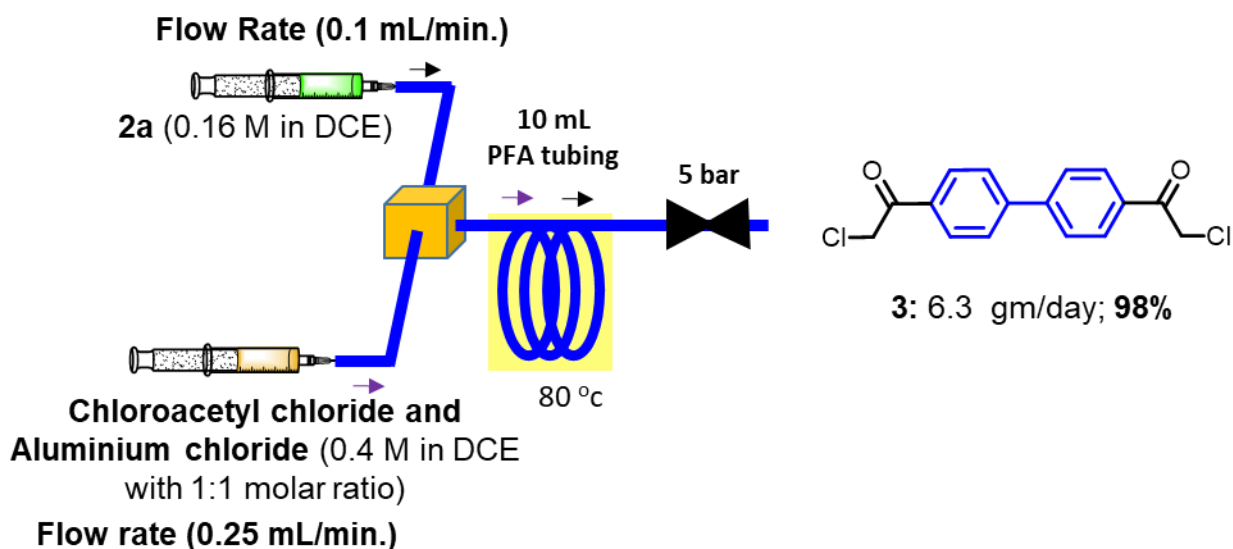
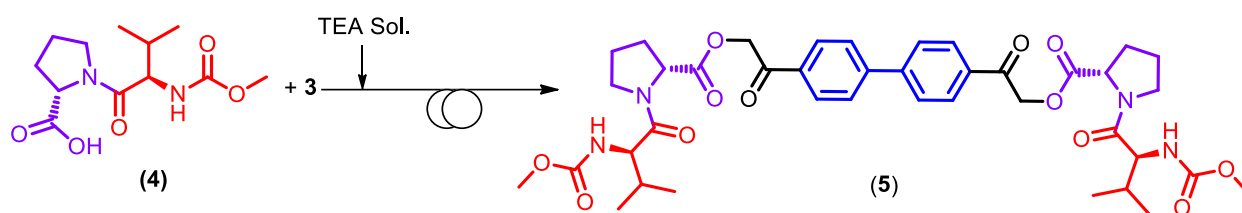


Figure S10. Schematic presentation of continuous micro-flow synthesis of daclatasvir API (**3**).

A solution of **2a** dissolved in DCE (0.16 M) and charged in one syringe. In another syringe filled with the solution of chloroacetyl chloride (0.4 M in DCE), and AlCl₃ (1 equiv.) (Fig.S10). The two solutions were introduced to a T-mixer in a flow rate with the ratio of 1: 6.25 (compound 2a: chloroacetyl chloride) to maintain the stoichiometry, and then passed through a PTFE tubing (id = 1000 μm, l = 12.8 m, vol. = 10 ml) to occur the Friedel-craft acylation during 28.6 min of residence time and 80 °C temperature and 5 bar pressure (Table S4, entry 5). The resulting solution was quenching with cold water and extracting through the regular process. ¹H NMR (400 MHz, CDCl₃) δ 8.14 – 8.04 (d, 4H), 7.84 – 7.73 (d, 4H), 4.74 (s, 4H). ¹³C NMR (126 MHz, CDCl₃) δ 190.66, 144.92, 133.85, 129.37, 127.80, 45.84. IR (ν_{max}): 2992, 2935, 1692, 1601, 1555, 1399, 1308, 1214, 966, 808, 765, 642 cm⁻¹; MS (EI): *m/z* 307.17 (M⁺).

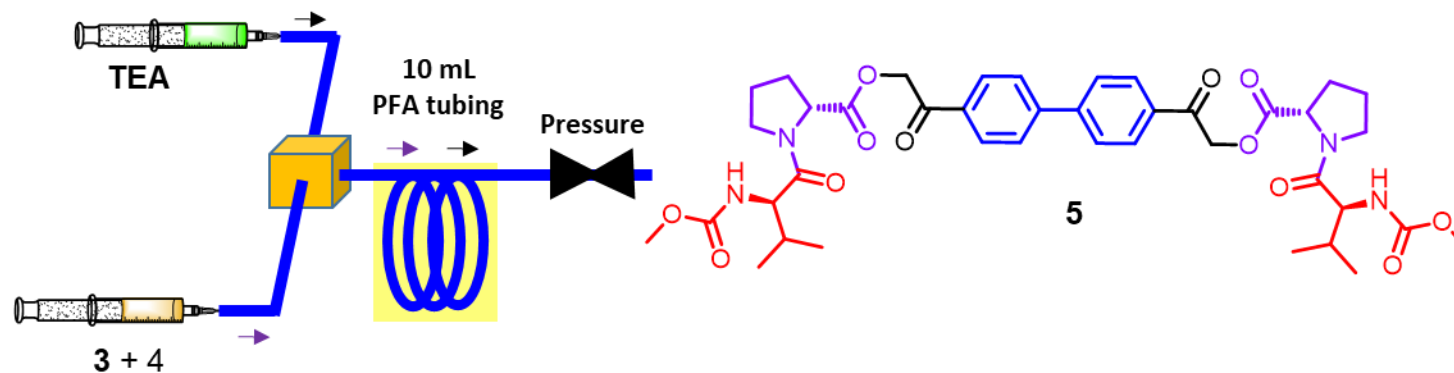
Step 2: Ester formation.



Reported batch method has been followed for the preparation of compound **4**. ¹⁴ ¹H NMR (400 MHz, CDCl₃) δ 10.17 (s, 1H), 5.94 (d, J = 9.4 Hz, 1H), 4.53 (dd, J = 8.4, 4.5 Hz, 1H), 4.27 (dd, J = 9.3, 7.5 Hz, 1H), 3.84 (dt, J = 9.6, 6.9 Hz, 1H), 3.70 – 3.65 (m, 1H), 3.63 (s, 3H), 2.23 – 2.14 (m, 1H), 2.15 – 1.96 (m, 4H), 0.99 (d, J = 6.7 Hz, 3H), 0.92 (d, J = 6.7 Hz, 3H). ¹³C NMR (100 MHz, CDCl₃) δ 174.82, 172.39, 157.51, 59.24, 57.94, 52.47, 47.73, 31.23, 28.86, 25.00, 19.26, 18.00.

A solution of compound **3** and **4** in MeCN was charged in one syringe and triethylamine in DCE was taken in another syringe (Fig. S11). The two solutions were introduced into a T-mixer in a varied flow rate and ratio to maintain the stoichiometry, and then passed through PTFE tubing for Friedel-craft acylation reaction. Optimization conditions were varied depending on the nature of the reagent, retention time, temperature, and pressure etc (Table S5).

Table S5. Optimization of continuous micro-flow reaction to synthesize daclatasvir intermediate API (5) in ultra-fast manner.



Entry	Flow rate (mL/min)		Temperature (°C)	Pressure (bar)	Retention time (min.)	Yield (%)
	Compound 3 + 4	TEA				
1	2.5	2.5	80	5	2	99
2	3.0	2.0	80	5	2	99
3	3.5	1.5	80	5	2	99
4	4.0	1.0	50	5	2	43

Reaction condition: (a) Stock solution **3** (0.25M in MeCN) + **4** (0.5M in MeCN); TEA (1.3M in MeCN); Yields are based on isolated yields.

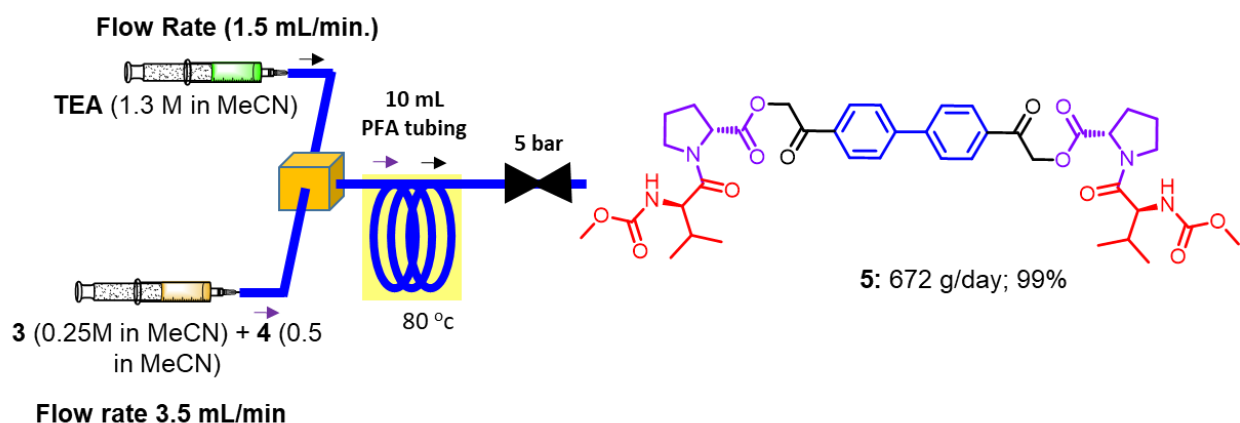
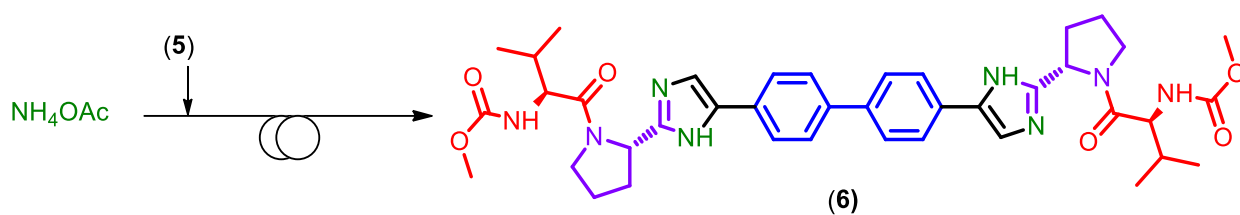


Fig. S11. Schematic presentation of continuous micro-flow synthesis of daclatasvir API (5).

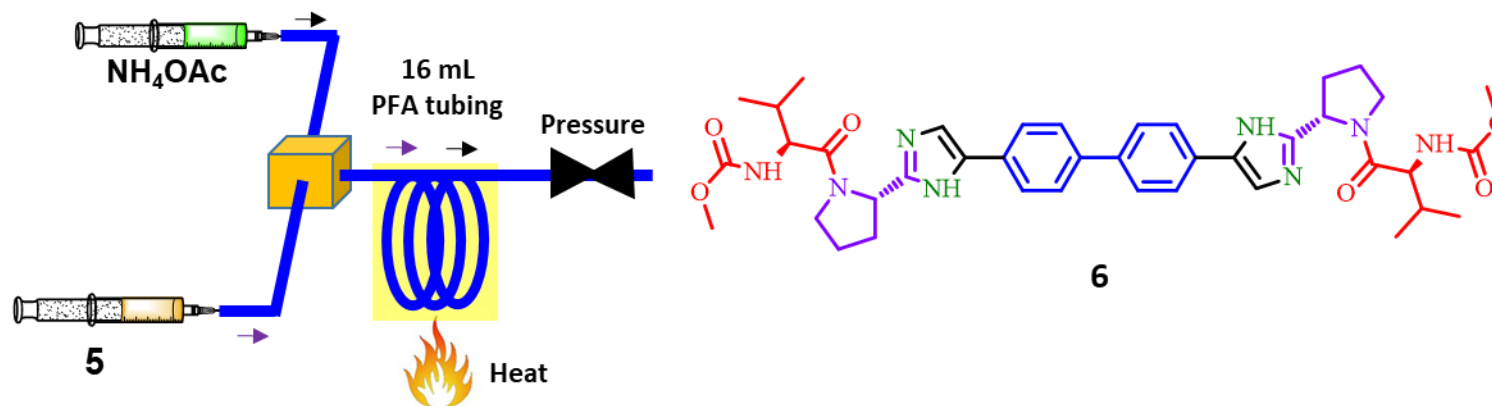
A reactant of **3** dissolved in MeCN (0.25 M) and mix with **4** (0.5 in MeCN) charged in one syringe. In another syringe filled with the solution of triethylamine (1.3 M in MeCN) (Fig. S11). The two solutions were introduced to a T-mixer in a flow rate with the ratio of 1: 2.25 (compound **4**: TEA) to maintain the stoichiometry, and then passed through a PTFE tubing (id = 1000 μm , l = 12.8 m, vol. = 10 ml) for the ester formation during 2 min of residence time and 80 °C temperature and 5 bar pressure (Table S5, entry 3). Under the stable condition, product was collected in reservoir containing cold water and extracting through the routine process. ^1H NMR (500 MHz, CDCl_3) 7.99 (t, J = 7.7 Hz, 2H), 7.72 (d, J = 8.3 Hz, 2H), 5.56 (d, J = 16.4 Hz, 1H), 5.40 (d, J = 9.3 Hz, 1H), 5.26 (d, J = 16.4 Hz, 1H), 4.71 (dd, J = 8.2, 5.1 Hz, 1H), 4.37 – 4.26 (m, 1H), 3.86 – 3.79 (m, 1H), 3.75 – 3.63 (m, 4H), 2.35 (ddd, J = 12.8, 9.8, 5.7 Hz, 2H), 2.24 – 2.15 (m, 1H), 2.11 – 2.03 (m, 2H), 1.01 (t, J = 13.6 Hz, 3H), 0.94 (t, J = 8.7 Hz, 3H). ^{13}C NMR (101 MHz, CDCl_3) δ 191.33, 171.41, 171.09, 157.09, 144.84, 133.55, 128.42, 127.72, 66.21, 58.70, 57.43, 52.24, 47.28, 31.24, 29.16, 24.93, 19.19, 17.50. IR (ν_{max}): 3384, 3304, 2964, 2883, 1751, 1703, 1641, 1518, 1434, 1370, 1230, 1170, 1100, 1034, 971, 816, 752, 667 cm^{-1} ; MS (EI): m/z 739.39 (M^+).

Step 3: Imidazole formation.



A solution of compound **5** in MeCN was taken in one syringe and ammonium acetate in MeCN was taken in another syringe (Table S6). The two solutions were introduced into a T-mixer in a varied flow rate and ratio to maintain the stoichiometry, and then passed through PTFE tubing for imidazole ring formation. Optimization conditions were varied depending on the nature of the reagent, retention time, temperature, and pressure etc.

Table S6. Optimization of continuous micro-flow reaction to synthesize daclatasvir API (**6**) in ultra-fast manner.



Entry	Flow rate (mL/min)		Temperature (°C)	Pressure (bar)	Retention time (min.)	Yield (%)
	Compound 5	NH ₄ OAc				
1	4.7	0.25	160	17	3.20	23
2	4.5	0.50	160	17	3.20	66
3	4.2	0.75	160	17	3.20	84
4	4.0	1.0	160	17	3.20	83
5	3.7	1.25	160	17	3.20	79
6	4.9	0.90	160	17	2.67	82
7	5.4	0.97	160	17	2.46	69

8	6.0	1.100	160	17	2.25	68
9	6.7	1.250	160	17	2.00	64
10	7.7	1.4	160	17	1.75	51
11	9.0	1.6	160	17	1.50	51

Reaction condition: stock solution **5** (0.16M in MeCN); NH₄OAc (8.6 in water); Yields are based on isolated yields.

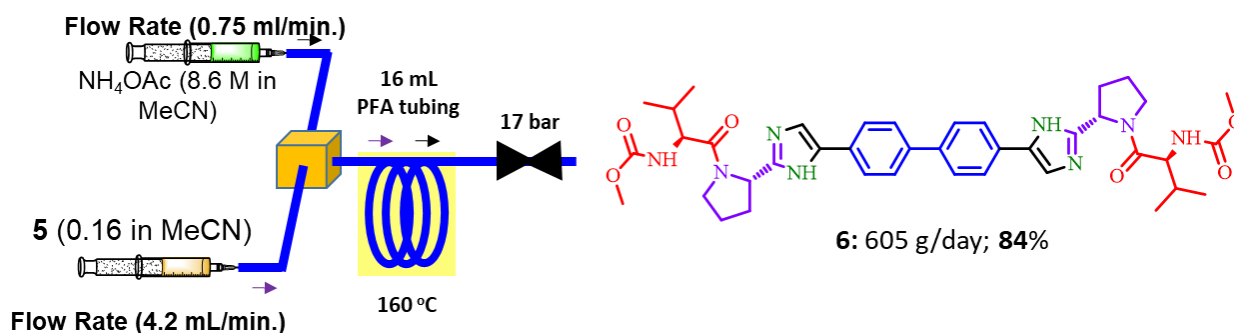


Fig. S12. Schematic presentation of continuous micro-flow synthesis of daclatasvir API (6).

The reactant **5** dissolved in MeCN (0.16 M) was charged in one syringe. In another syringe was taken solution of NH₄OAc (8.6 M in MeCN) (Fig. S12). The two solutions were introduced to a T-mixer in a flow rate with the ratio of 1: 9.6 (compound **5**: NH₄OAc) to maintain the stoichiometry, and then passed through a PTFE tubing (id = 1000 μm, l = 20.4 meter, vol. = 16 ml) to occur the ester formation during 3.2 min of residence time and 160 °C temperature and 17 bar pressure (Table S6, entry 3). The product was collected in reservoir containing cold water and extracted through the routine process.

¹H NMR (300 MHz, DMSO) δ 8.17 (s, 1H), 8.04 (d, *J* = 8.2 Hz, 2H), 7.94 (d, *J* = 8.4 Hz, 2H), 7.29 (d, *J* = 8.4 Hz, 1H), 5.22 (t, *J* = 6.8 Hz, 1H), 4.20 – 3.98 (m, 2H), 3.84 (s, 1H), 3.54 (s, 3H), 2.35 (dd, *J* = 20.1, 12.9 Hz, 1H), 2.28 – 1.96 (m, 4H), 0.99 – 0.81 (m, 3H), 0.77 (d, *J* = 6.6 Hz, 3H). ¹³C NMR (75 MHz, DMSO) δ 170.95, 156.93, 149.31, 139.14, 131.66, 127.15, 126.47, 125.86, 115.00, 31.03, 28.93, 24.89, 19.56, 17.71. IR (ν_{max}): 3283, 2964, 1707, 1628, 1524, 1441, 1361, 1246, 1189, 1106, 1035, 831, 755 cm⁻¹. MS (EI): *m/z* 738.39 (M⁺).^{S15}

5. Spectra

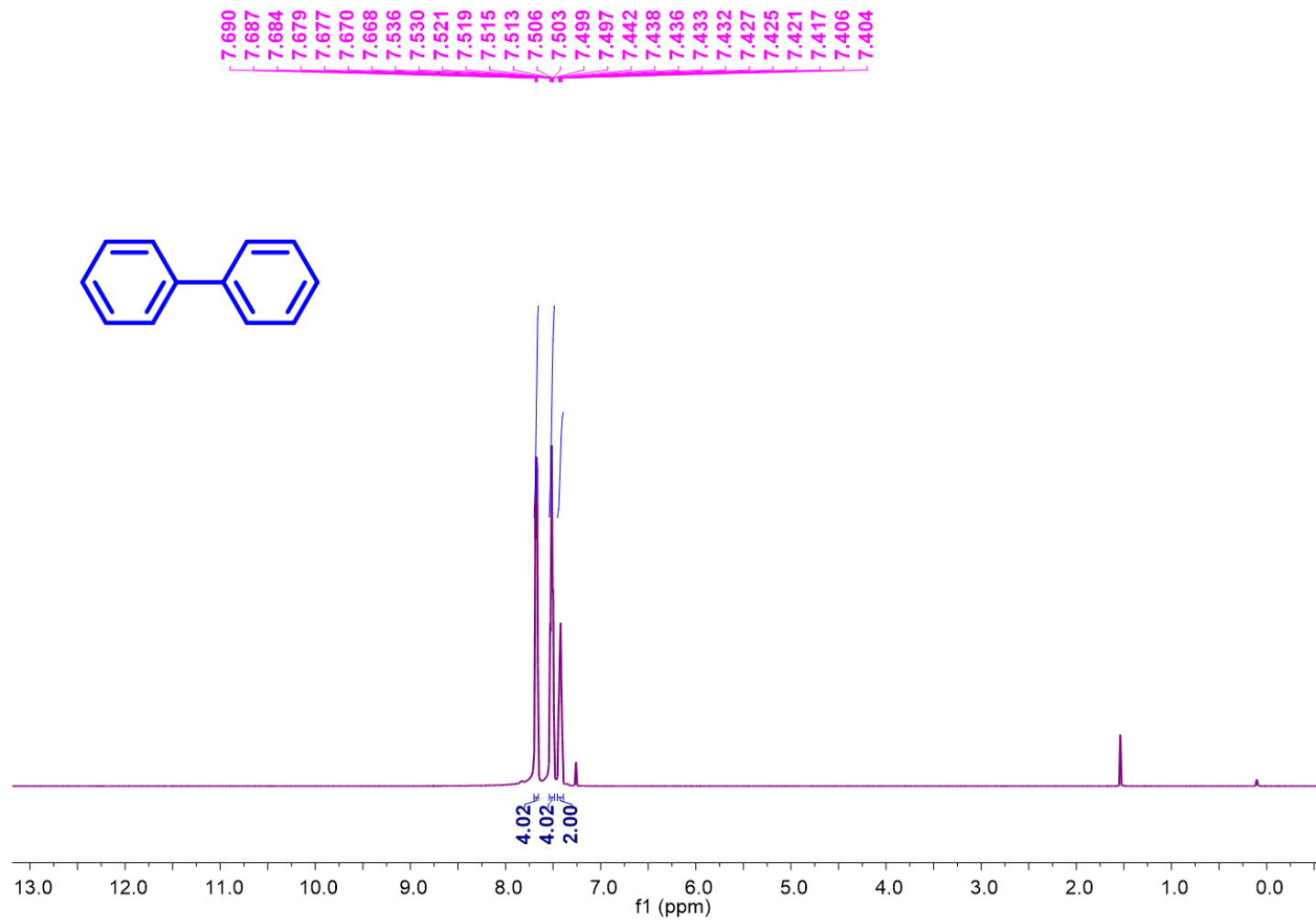


Fig. S13. ¹H NMR spectra of biphenyl (**2a**) in CDCl₃.

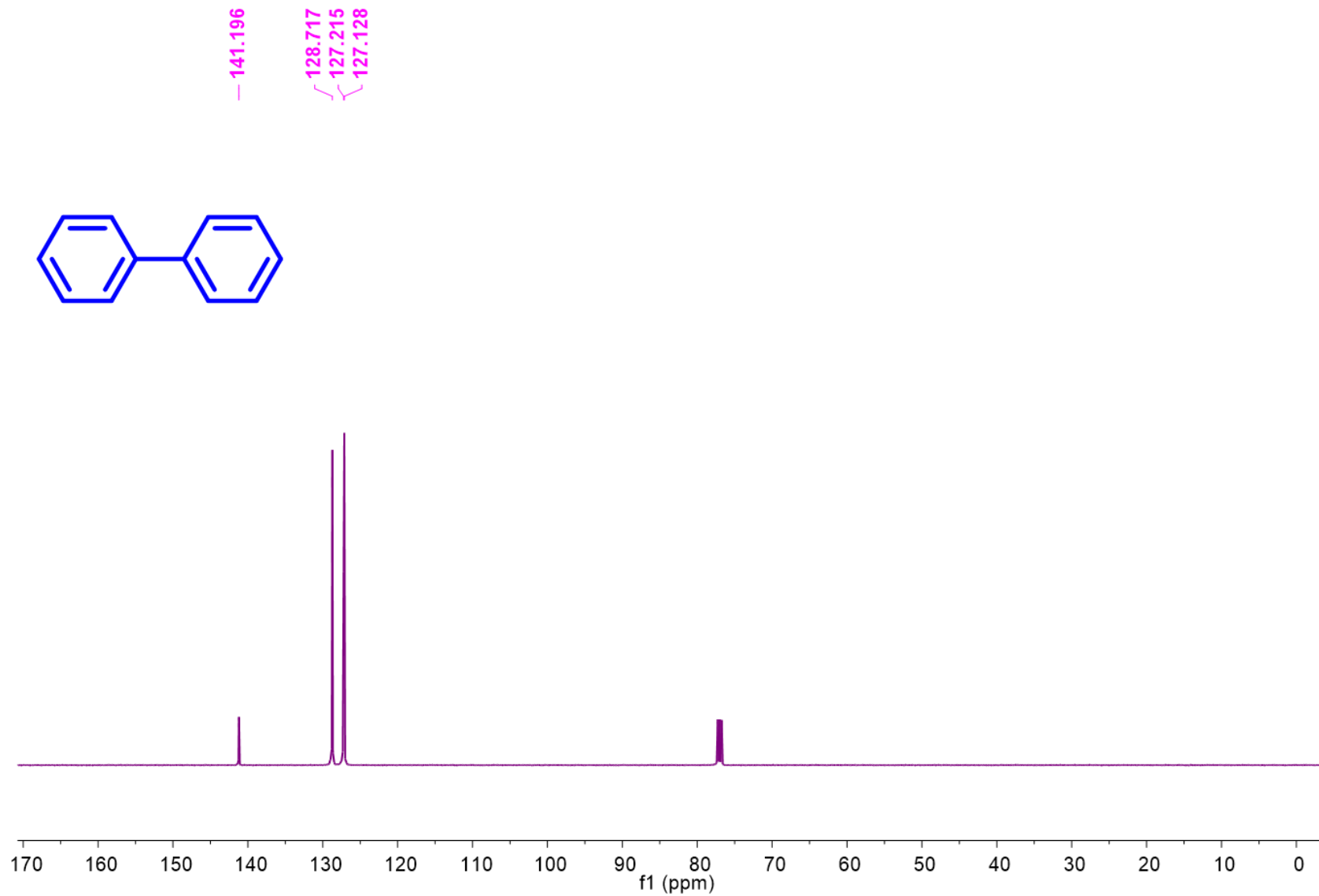


Fig. S14. ¹³C NMR spectra of biphenyl (**2a**) in CDCl₃.

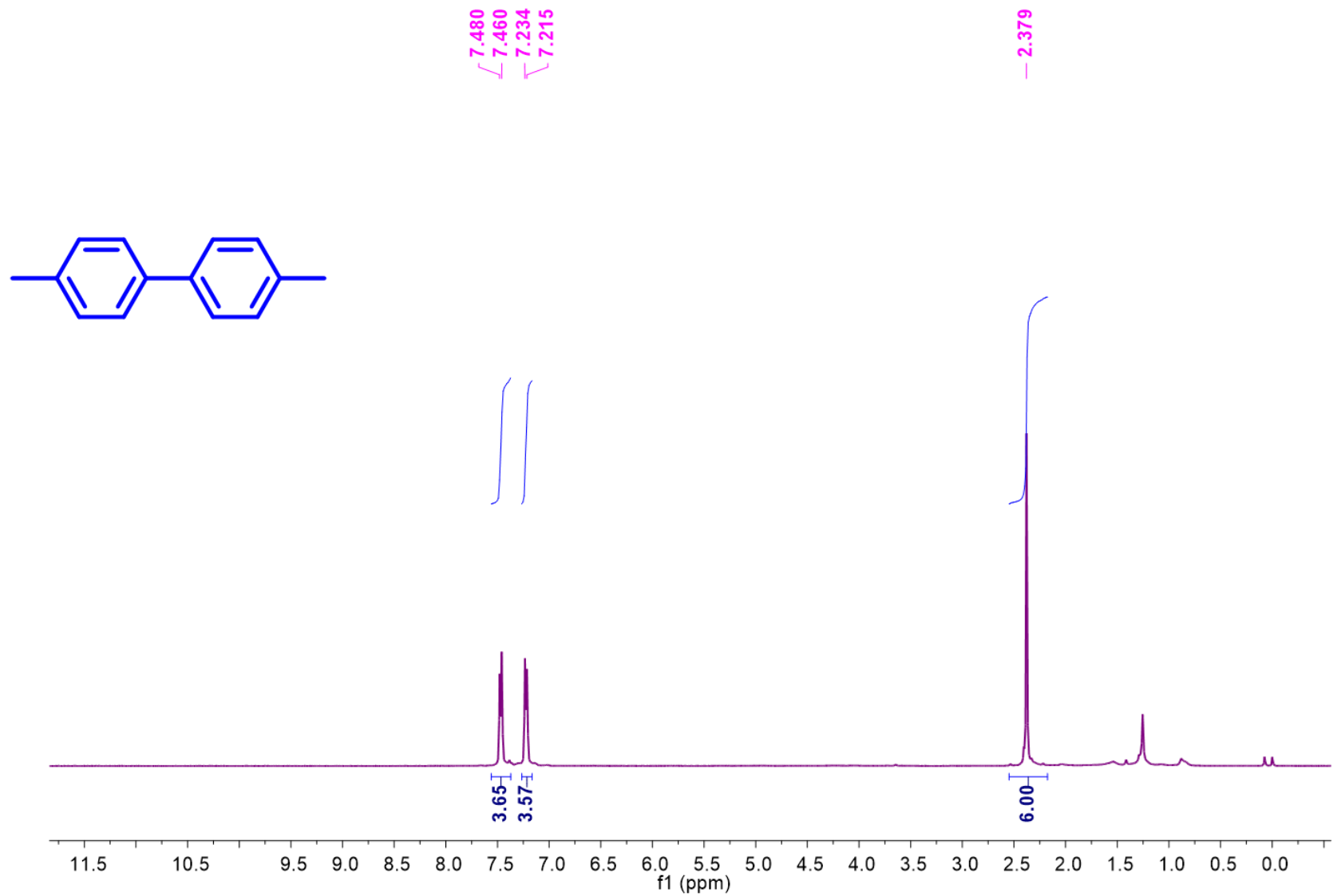


Fig. S15. ¹H NMR spectra of 4,4'-dimethyl-1,1'-biphenyl (**2b**) in CDCl₃.

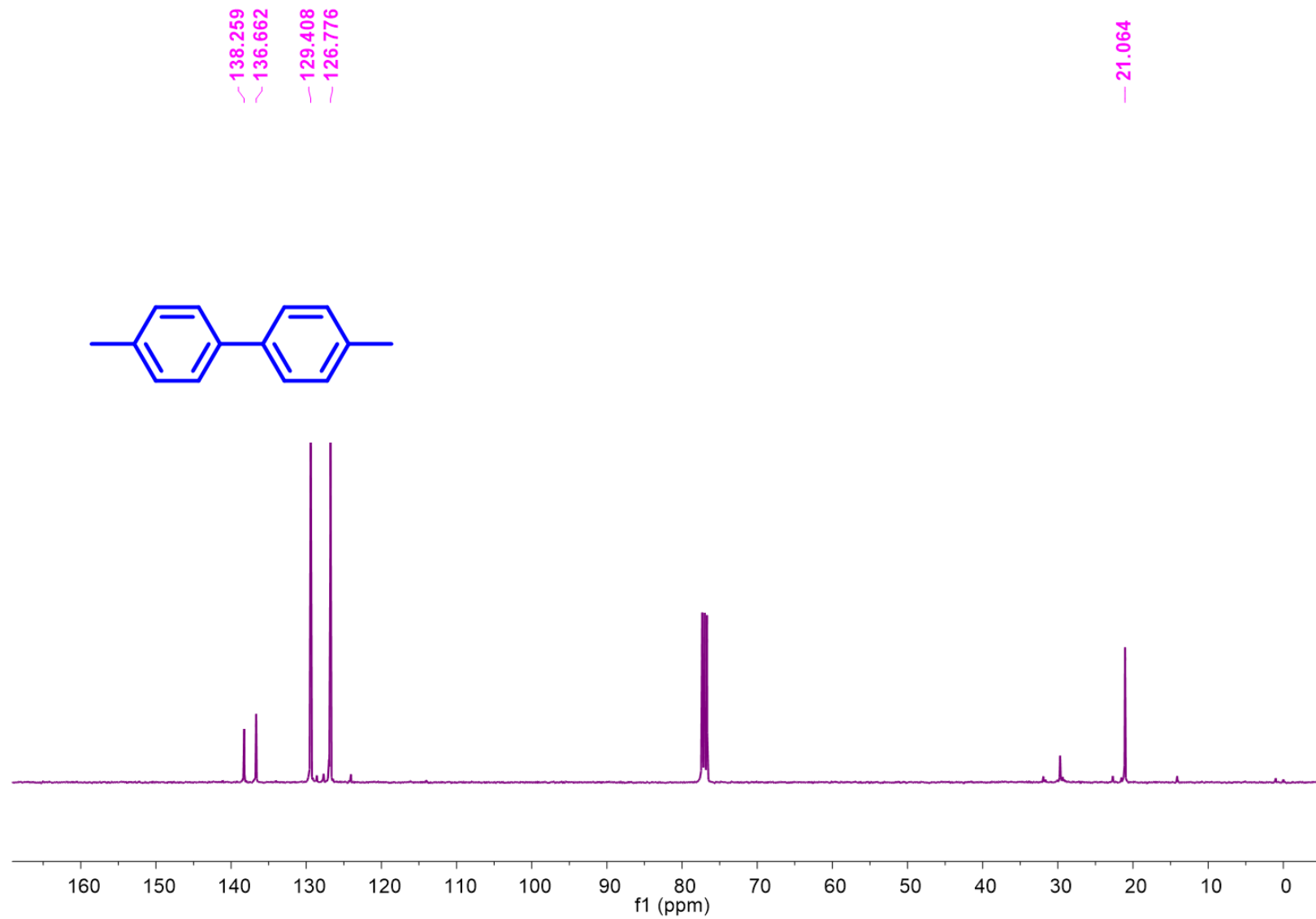


Fig.S16. ^{13}C NMR spectra of 4,4'-dimethyl-1,1'-biphenyl (**2b**) in CDCl_3 .

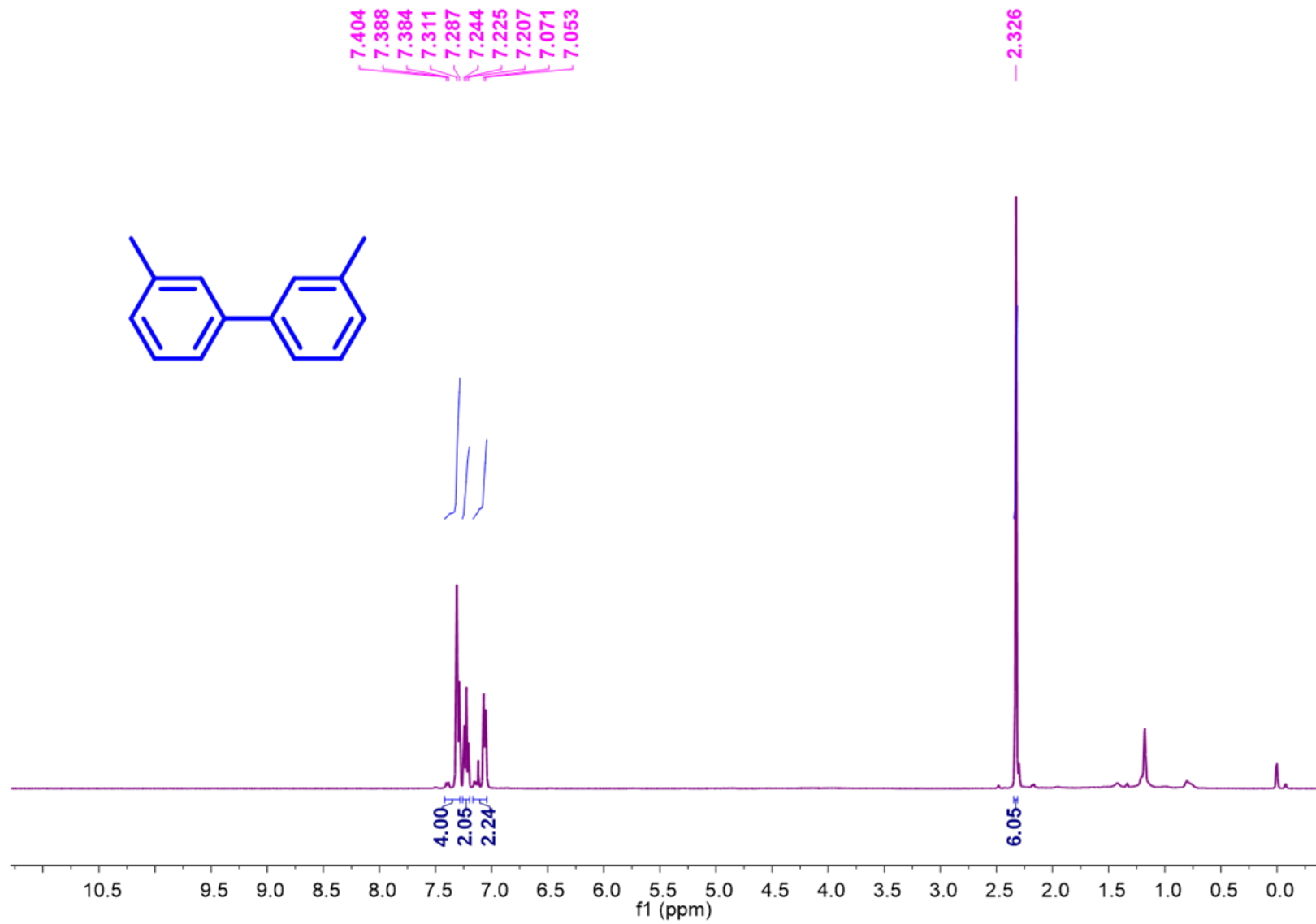


Fig. S17. ¹H NMR spectra of 3,3'-dimethyl-1,1'-biphenyl (**2c**) in CDCl₃.

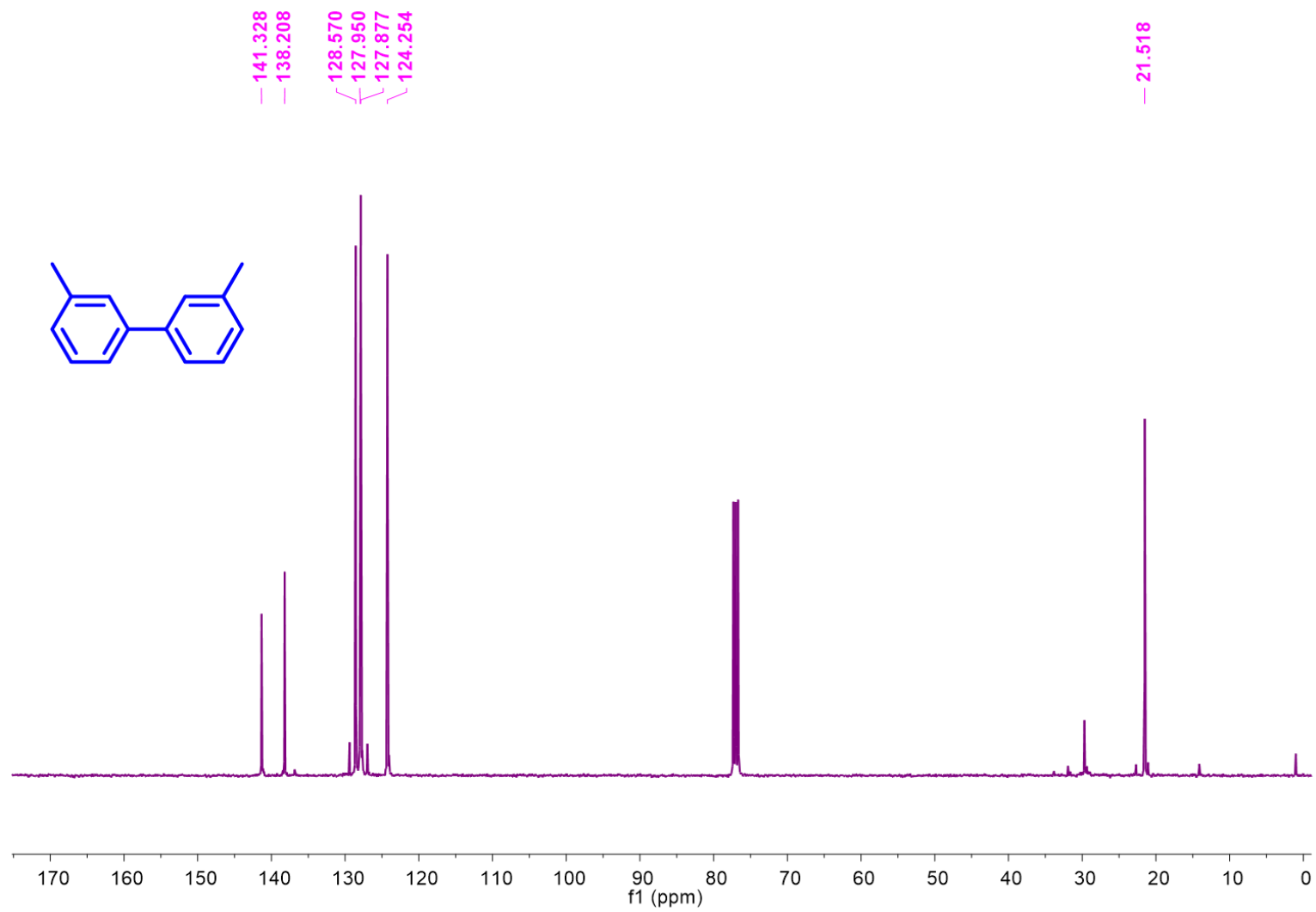


Fig. S18. ¹³C NMR spectra of 3, 3'-dimethyl-1,1'-biphenyl (**2c**) in CDCl₃.

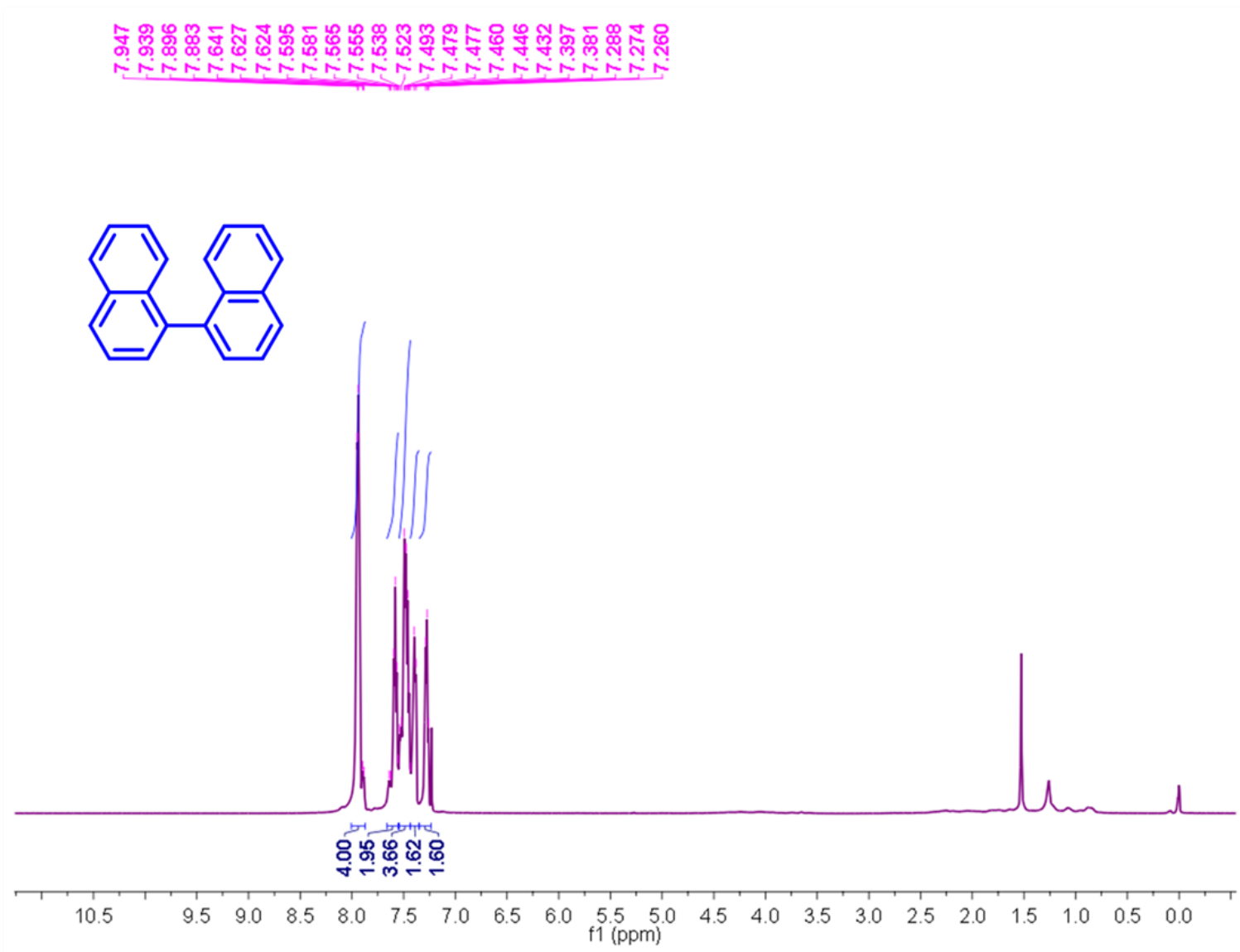


Fig. S19. ¹H NMR spectra of 1,1'-binaphthalene (**2d**) in CDCl₃.

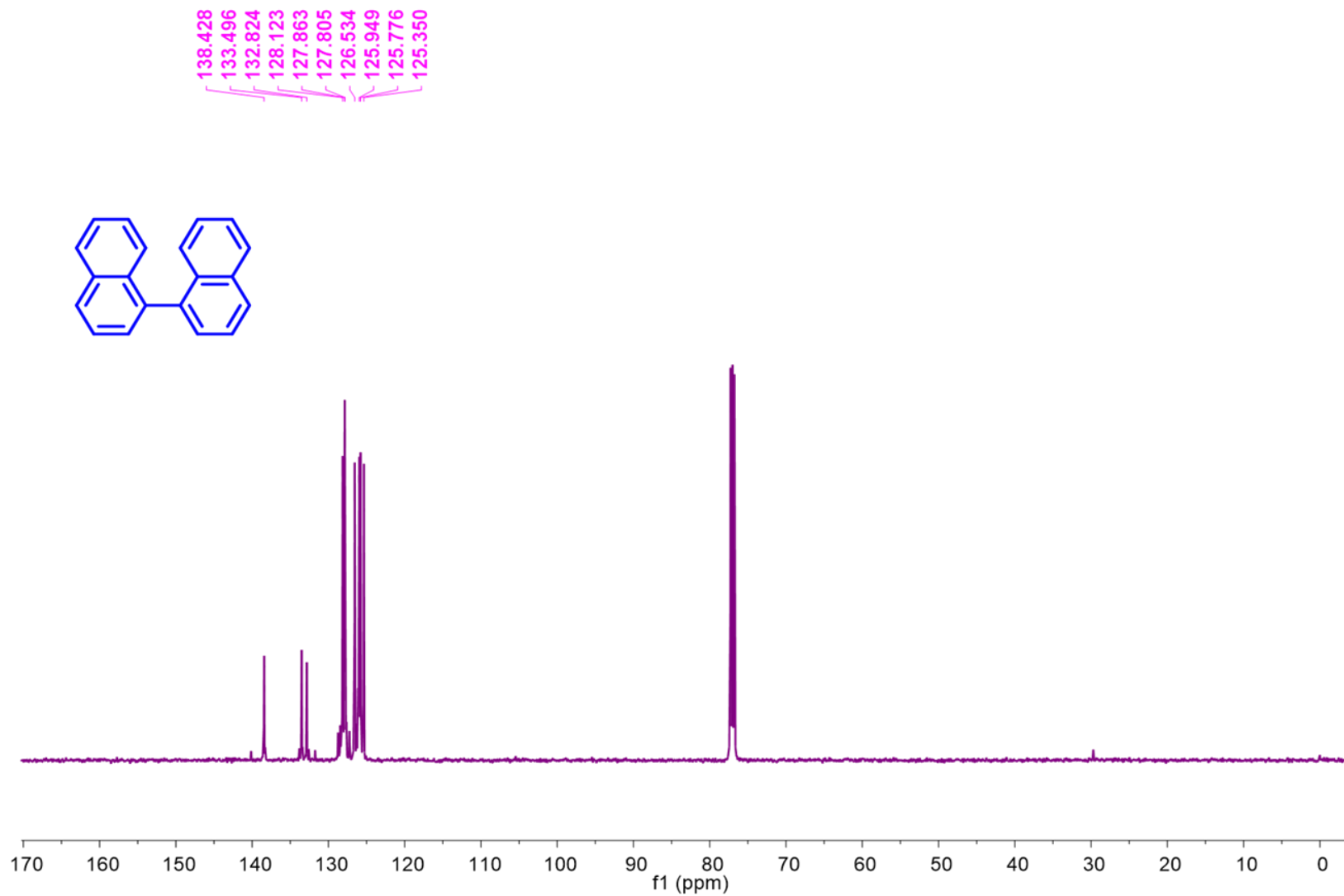


Fig. S20. ^{13}C NMR spectra of 1,1'-binaphthalene (**2d**) in CDCl_3 .

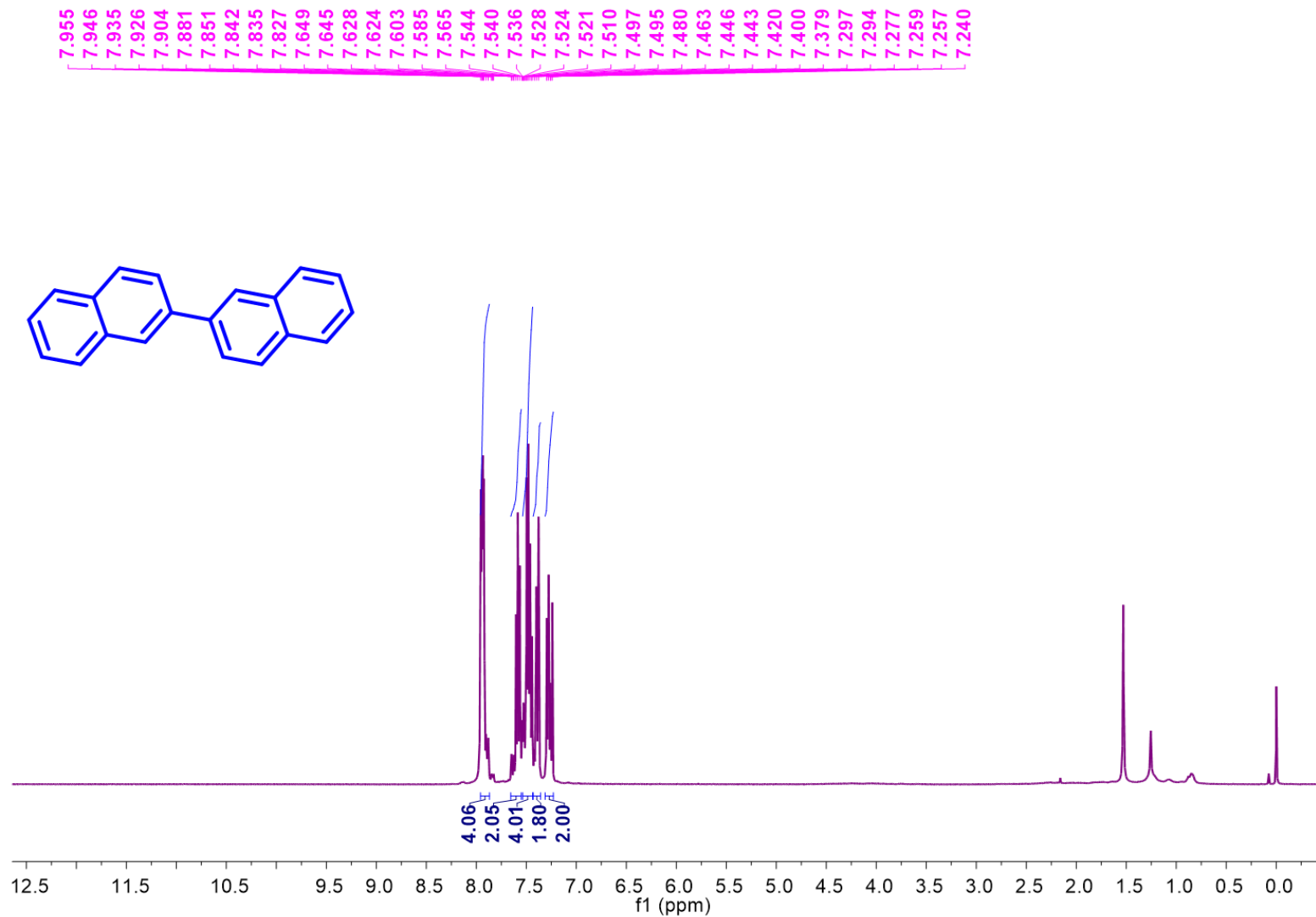


Fig. S21. ¹H NMR spectra of 2,2'-binaphthalene (**2e**) in CDCl₃.

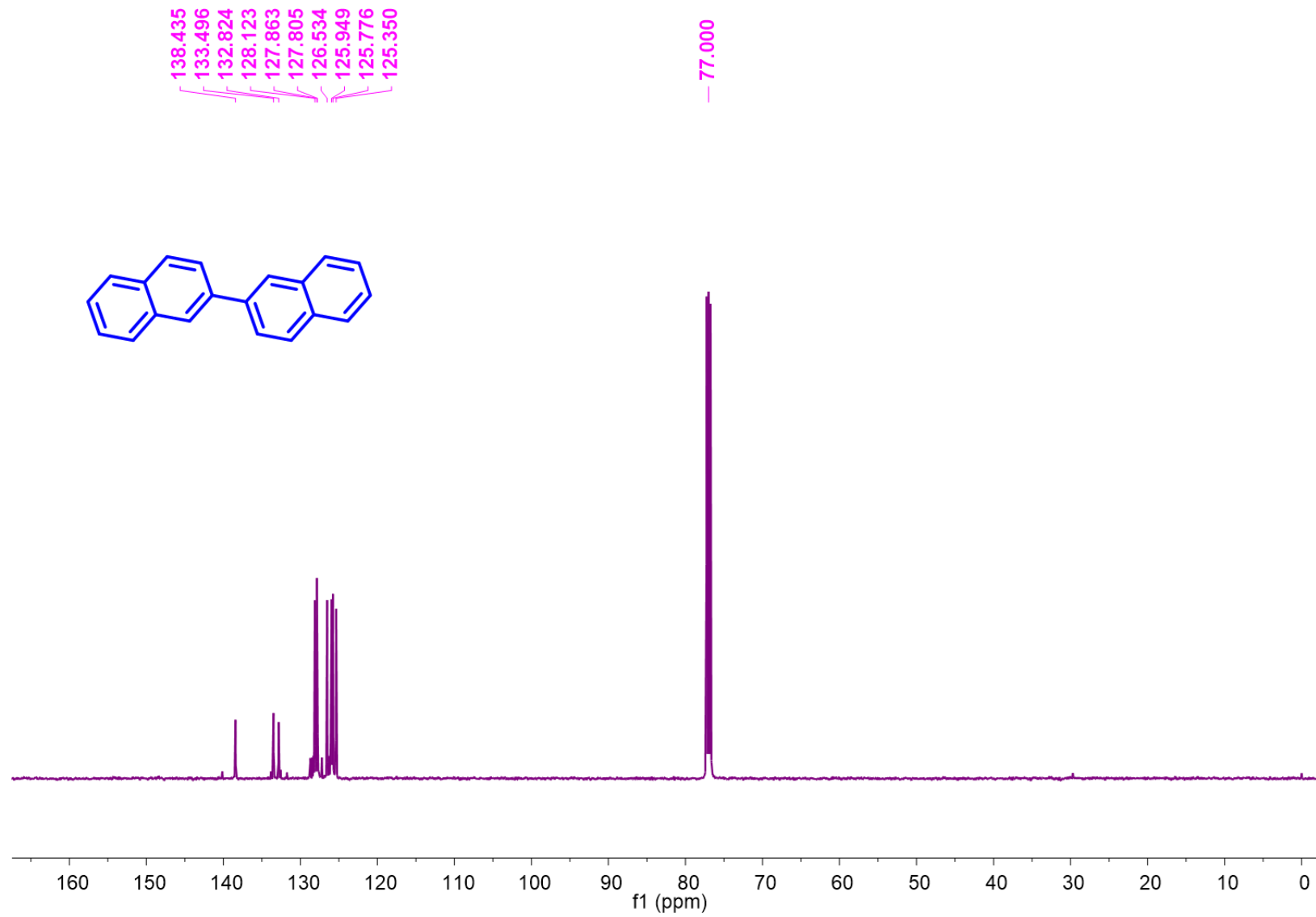


Fig. S22. ^{13}C NMR spectra of 2,2'-binaphthalene (**2e**) in CDCl_3 .

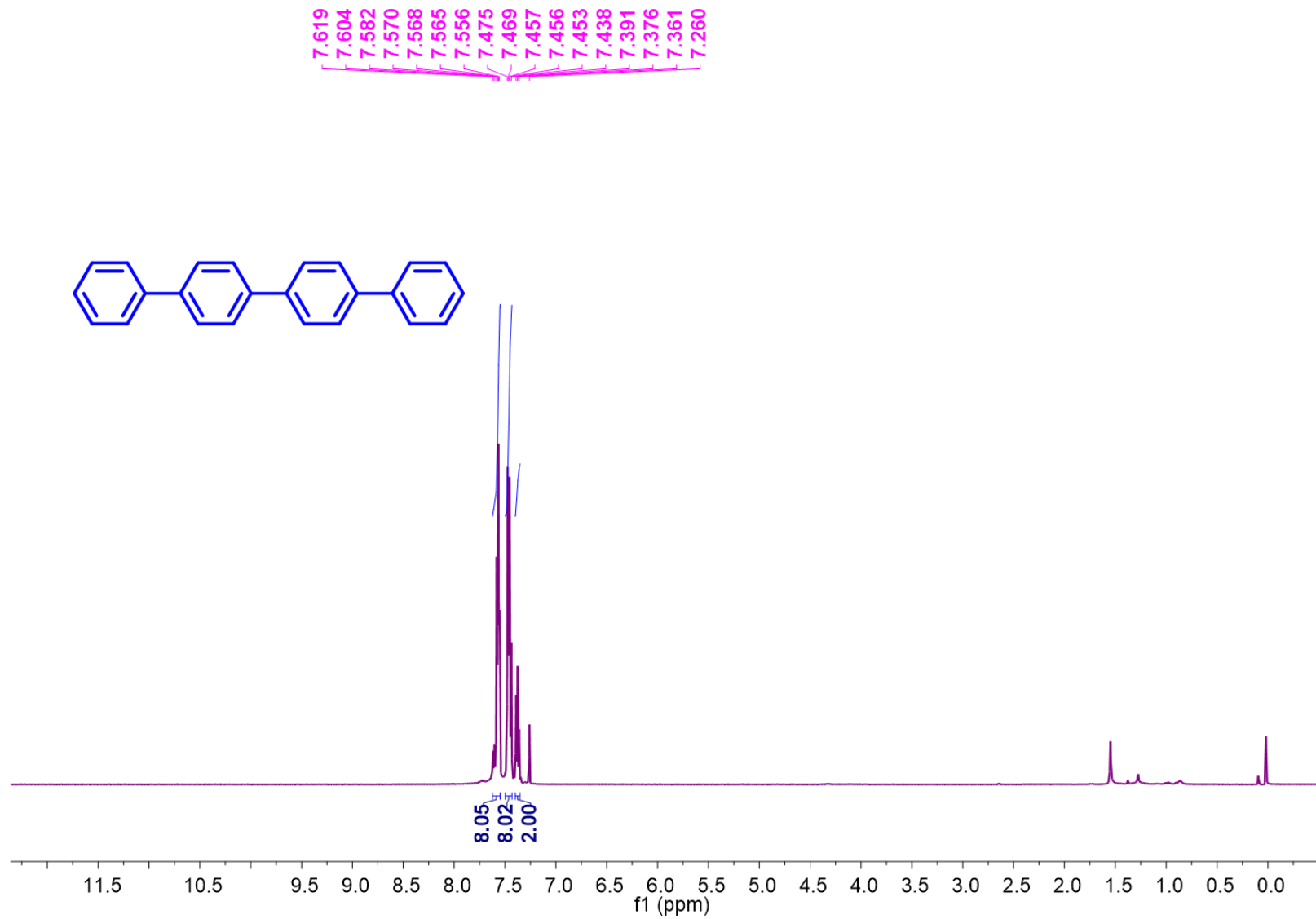


Fig. S23. ^1H NMR spectra of 1, 1':4', 1'':4'', 1''':4'''-quaterphenyl (**2f**) in CDCl_3 .

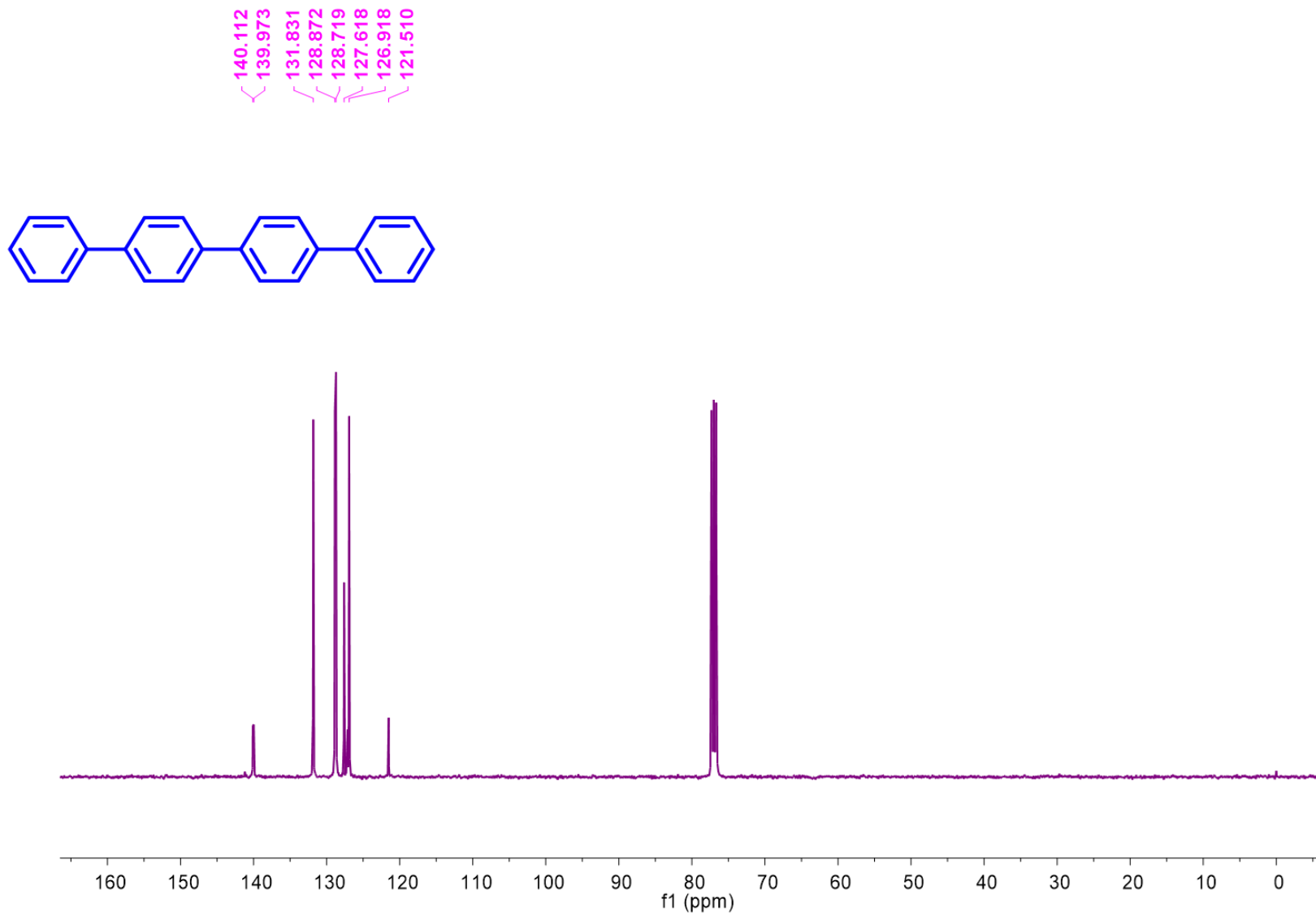


Fig. S24. ¹³C NMR spectra of 1, 1':4', 1'':4'', 1''':4'''-quaterphenyl (**2f**) in CDCl₃.

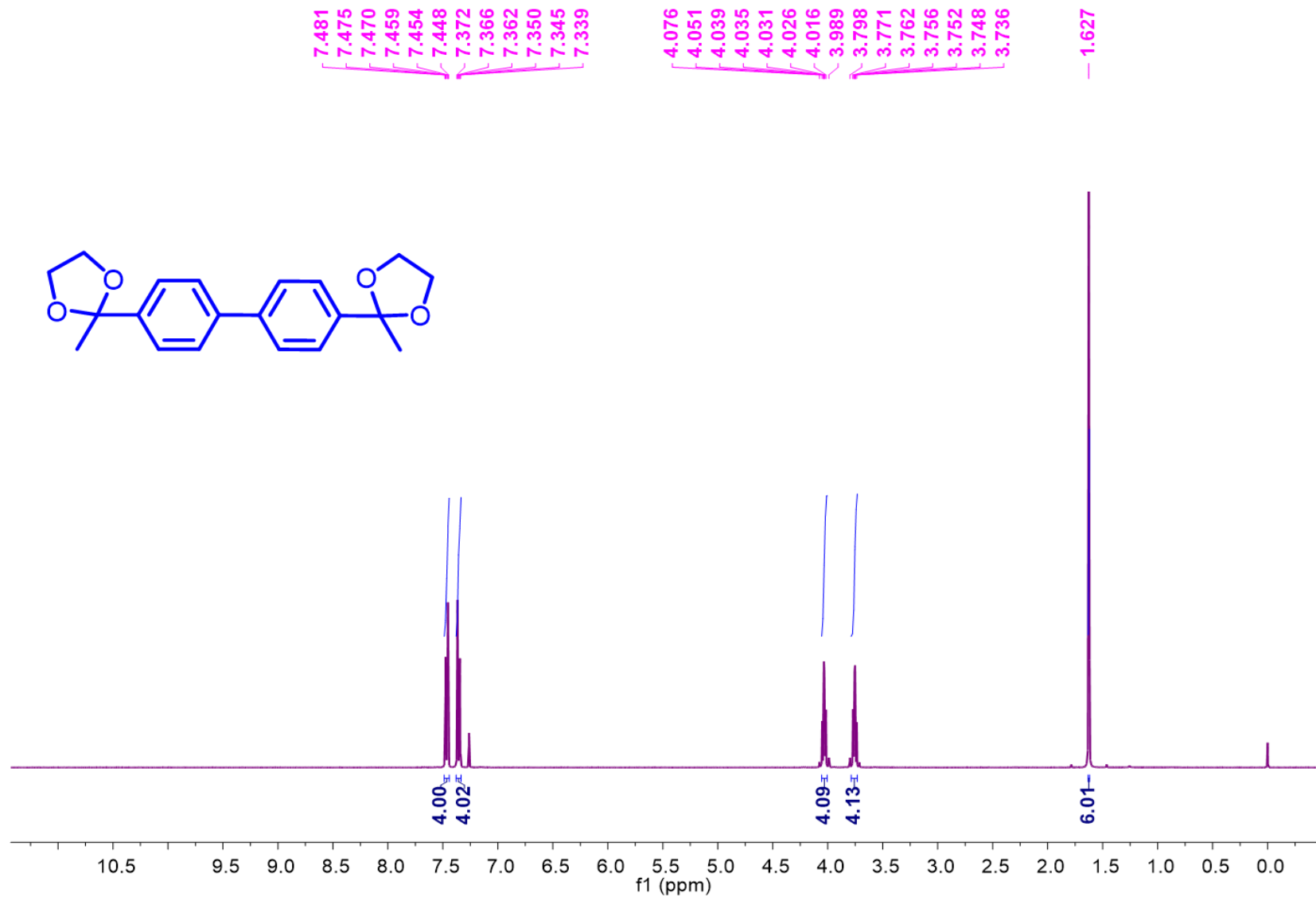


Fig. S25. ¹H NMR spectra of 1,1'-([1,1'-biphenyl]-4,4'-diyl) diethanone (**2g**) in CDCl₃.

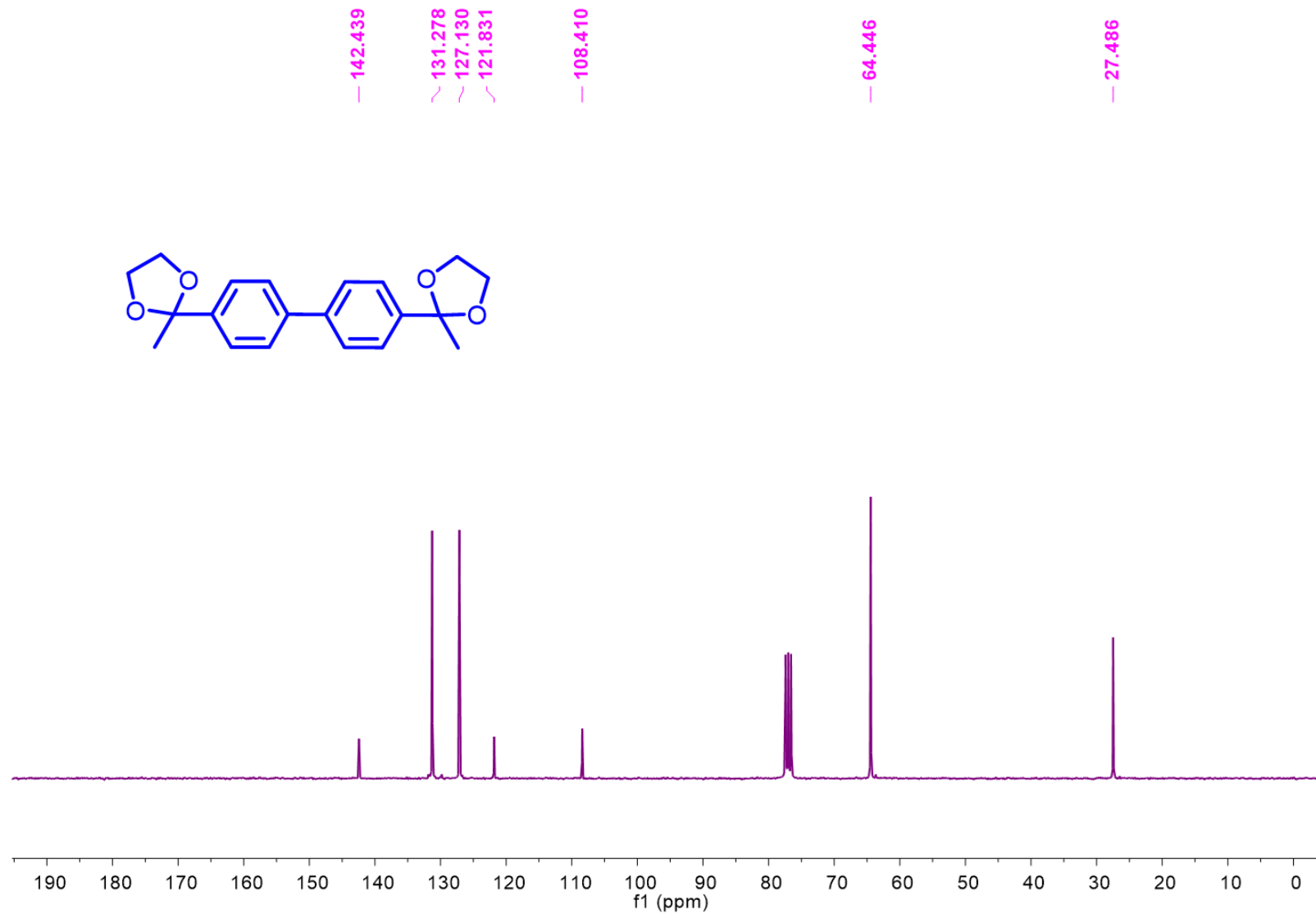


Fig. S26. ¹³C NMR spectra of 1,1'-([1,1'-biphenyl]-4,4'-diyl) diethanone (**2g**) in CDCl₃.

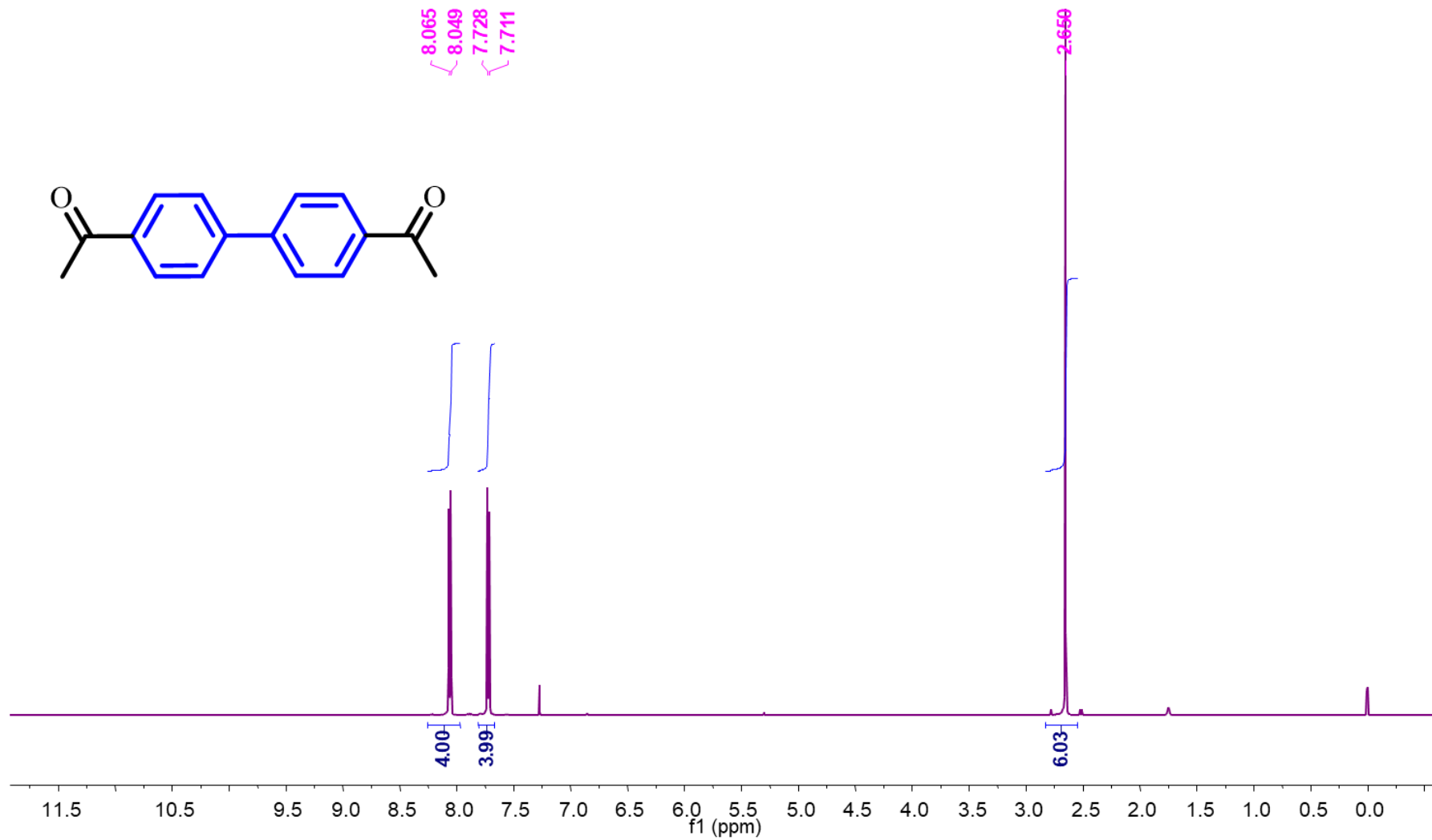


Fig. S27. ¹H NMR spectra of 1,1'-([1,1'-biphenyl]-4,4'-diyl) diethanone (**2h**) in CDCl₃.

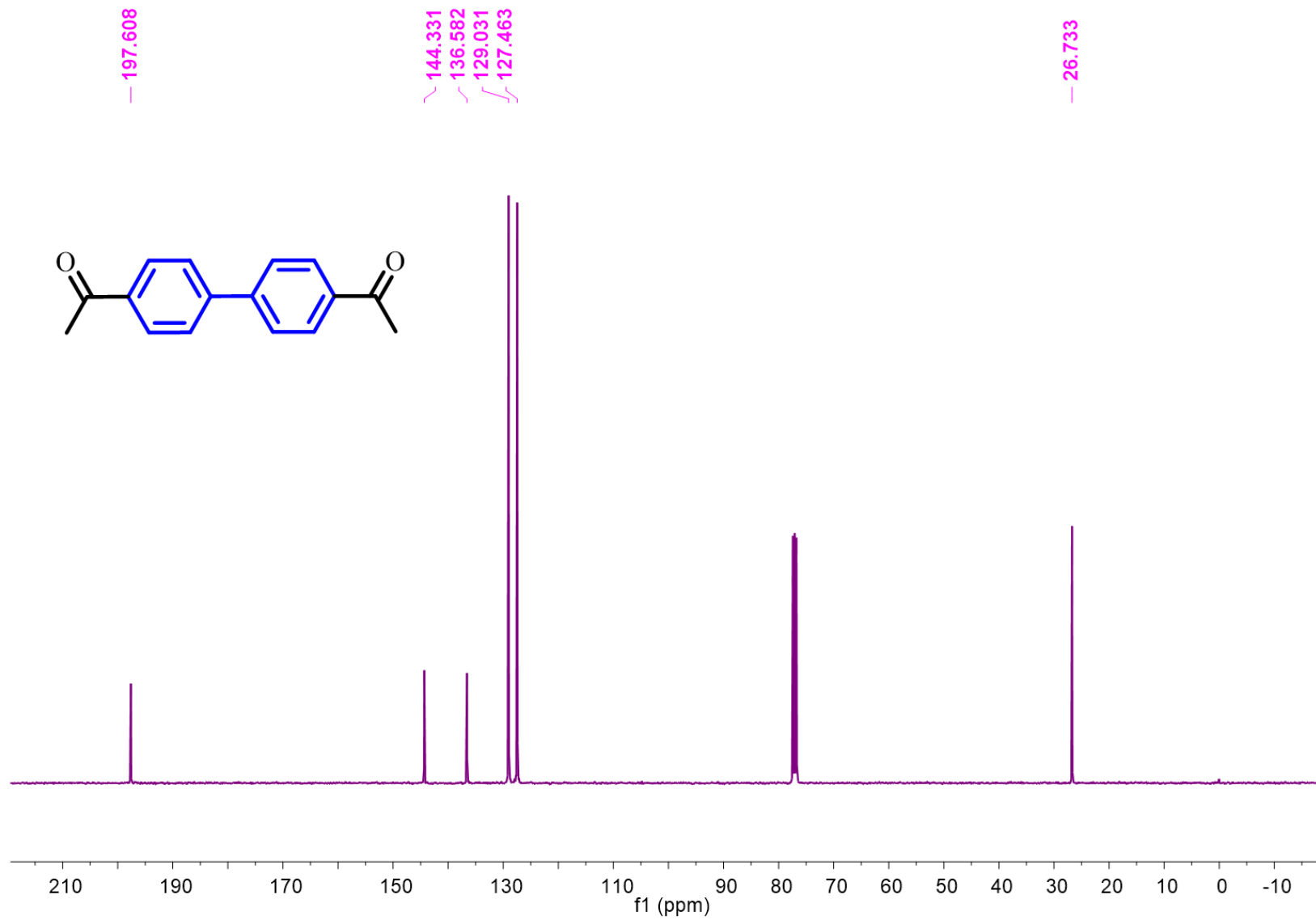


Fig. S28. ¹³C NMR spectra of 1,1'-([1,1'-biphenyl]-4,4'-diyl) diethanone (**2h**) in CDCl₃.

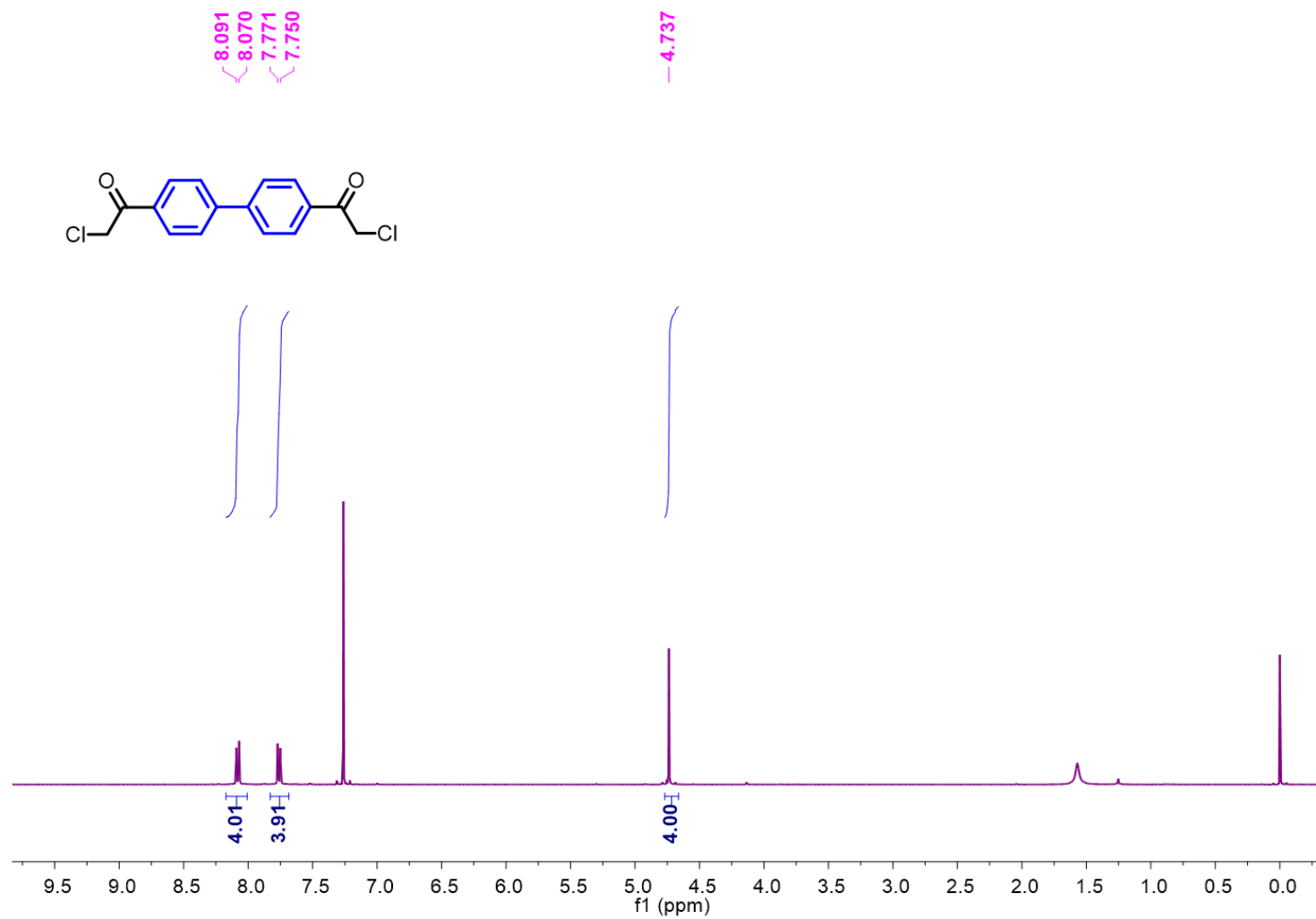


Fig. S29. ¹H NMR spectra of 1, 1'-([1, 1'-biphenyl]-4, 4'-diyl)bis(2-chloroethan-1-one) (**3**) in CDCl₃.

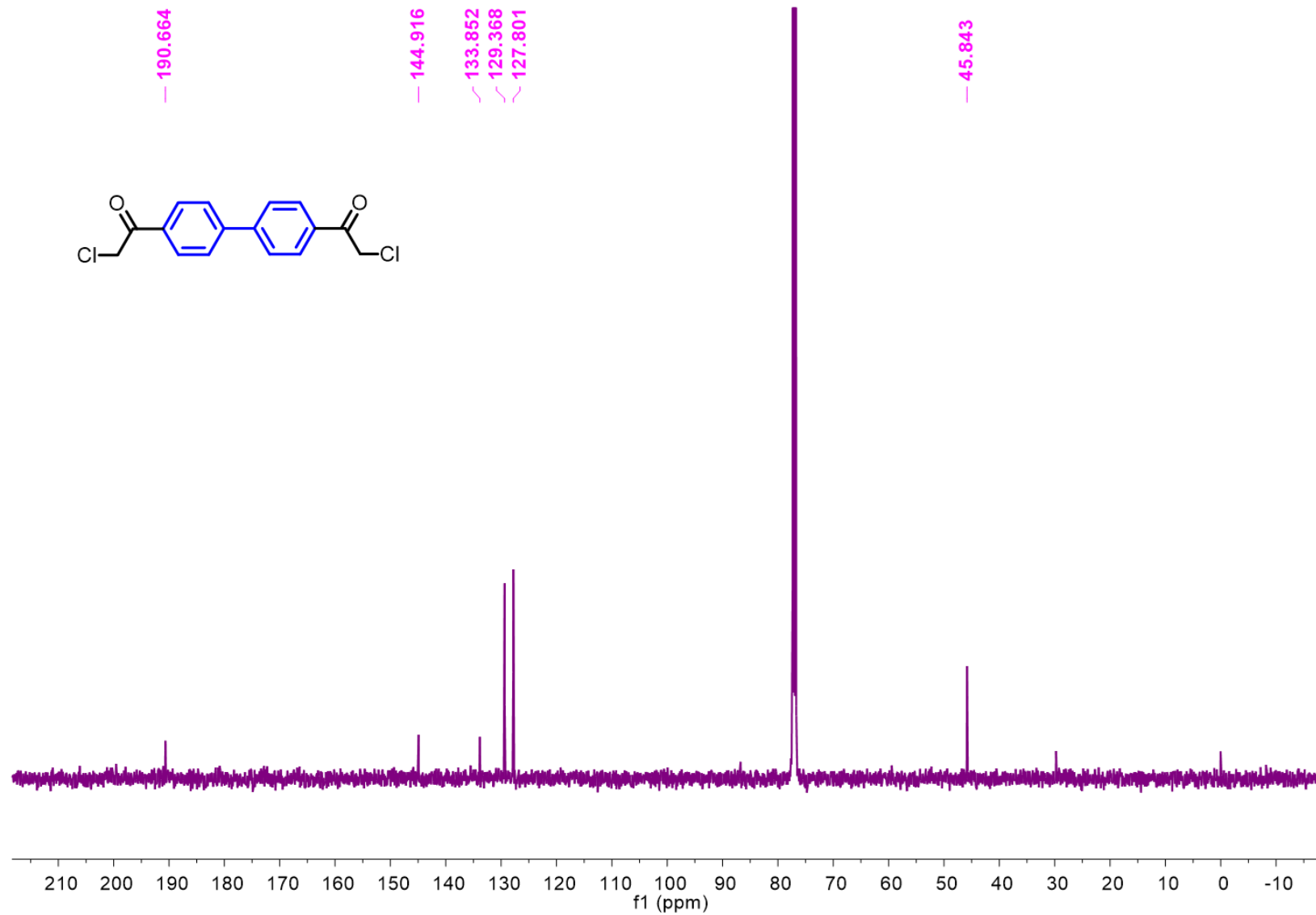


Fig. S30. ¹³C NMR spectra of 1, 1'-([1,1'-biphenyl]-4, 4'-diyl)bis(2-chloroethan-1-one) (**3**) in CDCl₃.

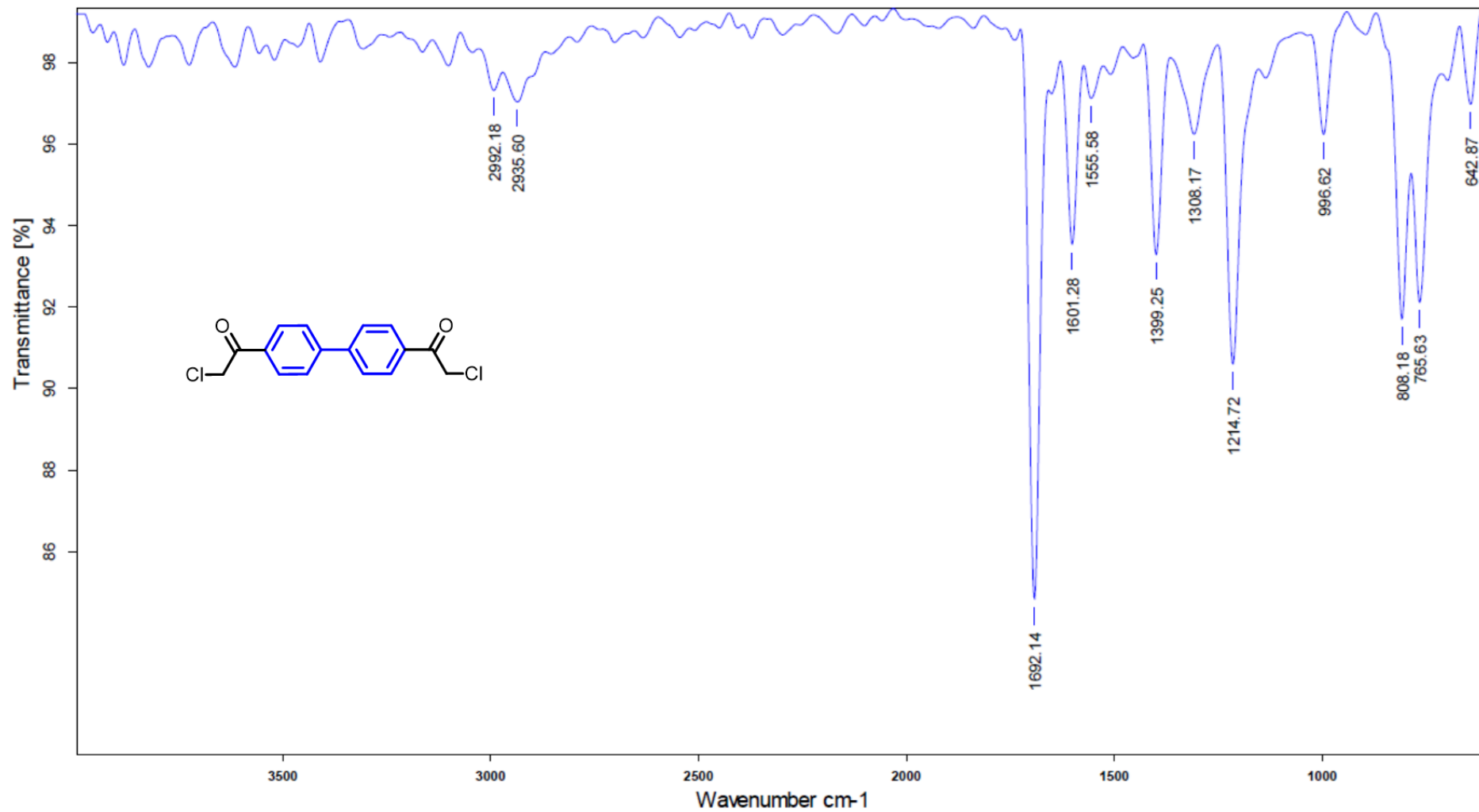
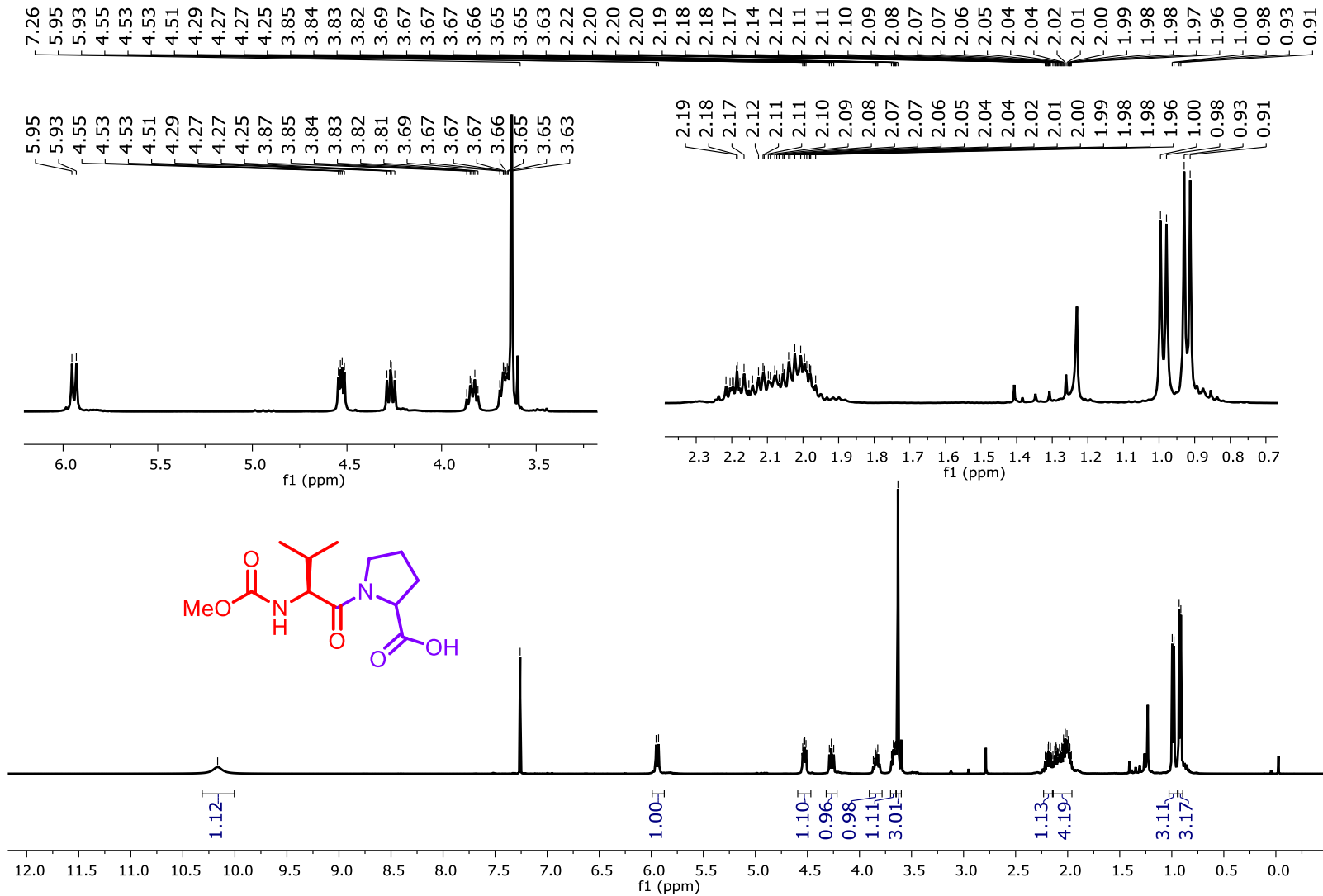


Fig. S31. IR spectra of 1, 1'-([1, 1'-biphenyl]-4, 4'-diyl)bis(2-chloroethan-1-one) (**3**).



14-NPL-09-SG-RK-29-1-19-1H acid

Fig. S32. ¹H NMR spectra of 1-((S)-2-((methoxycarbonyl)amino)-3-methylbutanoyl)pyrrolidine-2-carboxylic acid (**4**).

15-27-SG-RK-29-1-19-13C

~ 174.82
~ 172.39

— 157.51

{ 77.55
77.23
76.91

~ 59.24
~ 57.94
~ 52.47
~ 47.73

~ 31.23
~ 28.86
~ 25.00
~ 19.26
~ 18.00

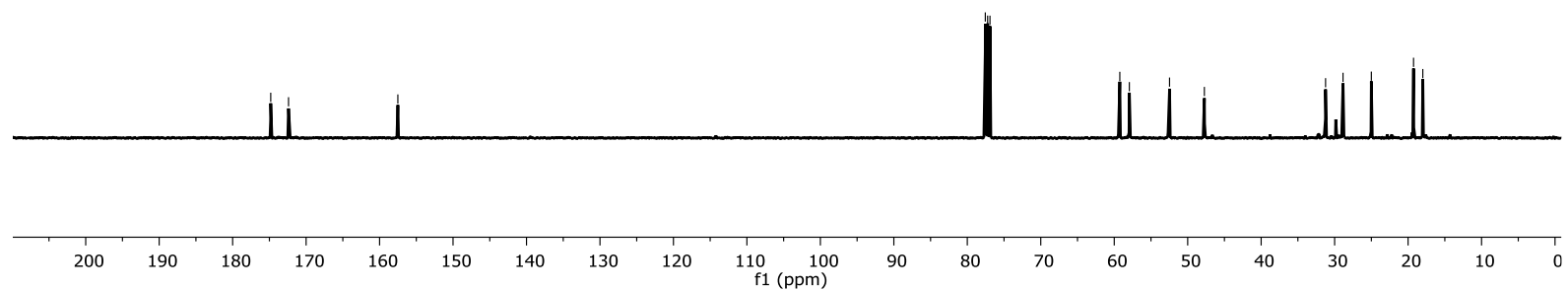
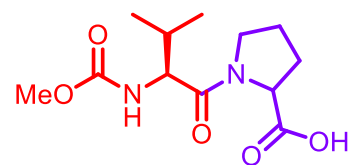


Fig. S33. ^{13}C NMR spectra of 1-((*S*)-2-((methoxycarbonyl)amino)-3-methylbutanoyl)pyrrolidine-2-carboxylic acid (**4**).

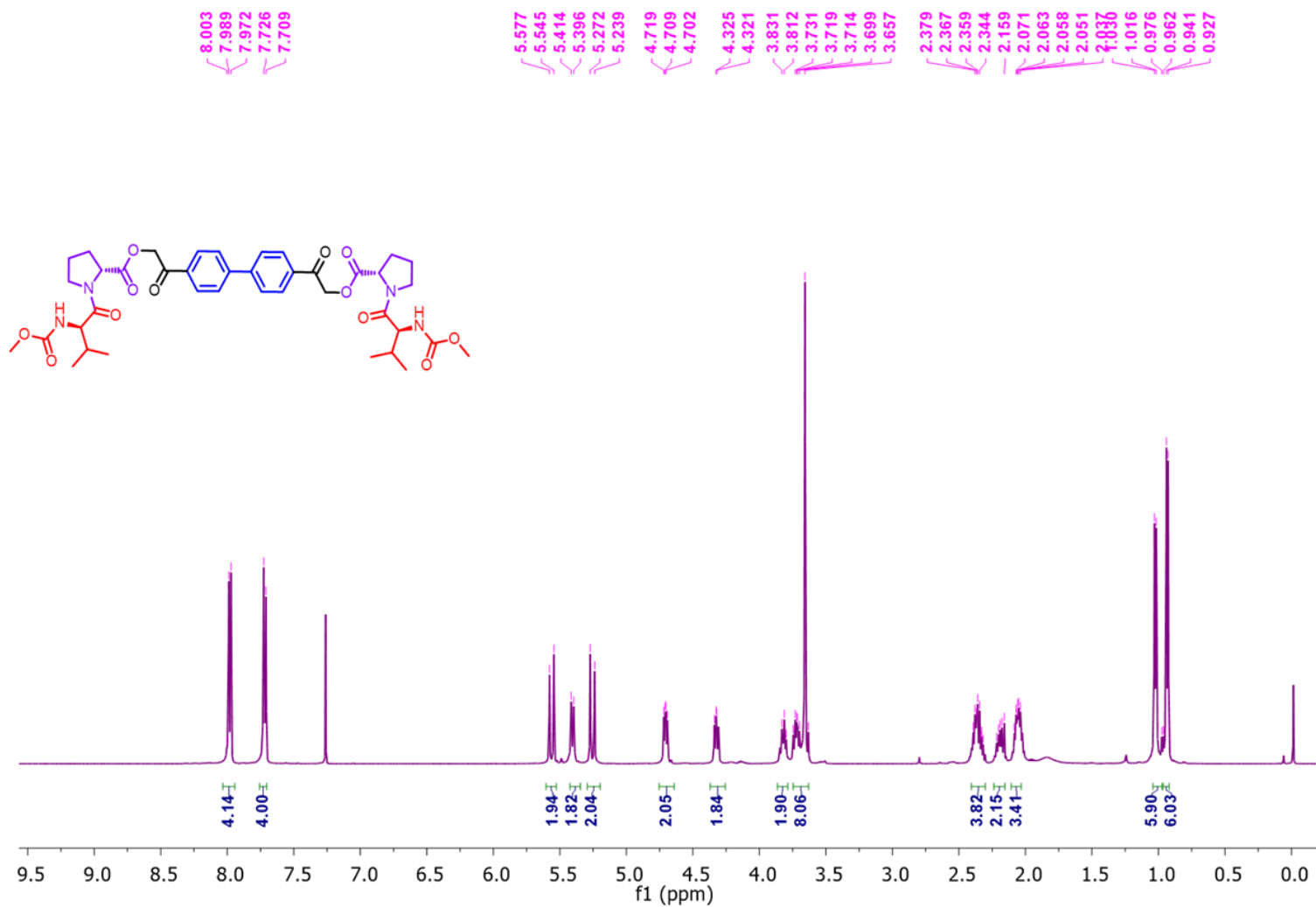


Fig. S34. ¹H NMR spectra of 2-(4'-(2-(((methoxycarbonyl)-D-valyl-D-prolyl)oxy)acetyl)-[1, 1'-biphenyl]-4-yl)-2-oxoethyl (methoxycarbonyl)-L-valyl-L-prolinate (**5**) in CDCl₃.

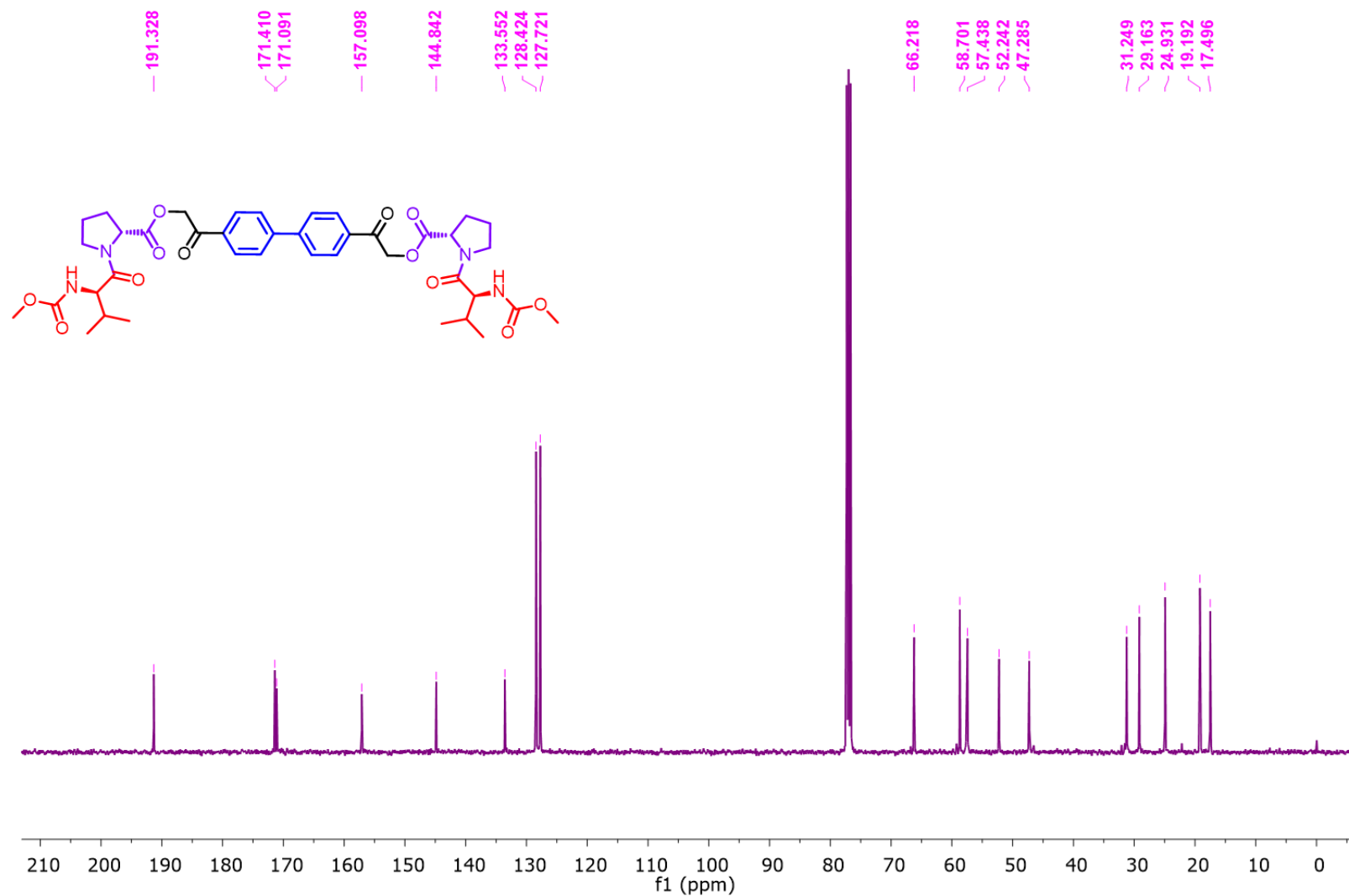


Fig. S35. ¹³C NMR spectra of 2-(4'-(2-(((methoxycarbonyl)-D-valyl-D-prolyl)oxy)acetyl)-[1, 1'-biphenyl]-4-yl)-2-oxoethyl (methoxycarbonyl)-L-valyl-L-prolinate (**5**) in CDCl₃.

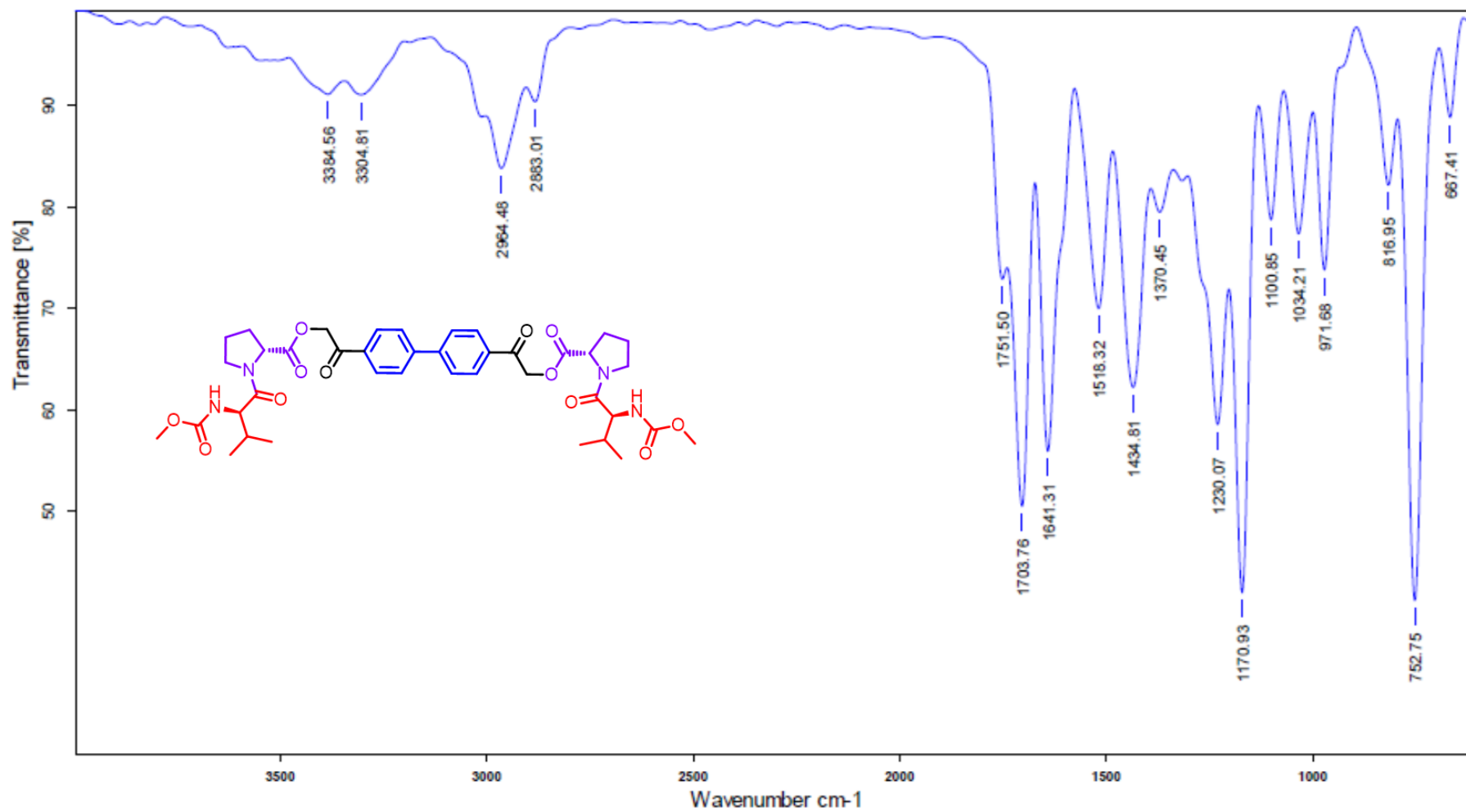


Fig. S36. IR spectra of 2-(4'-(2-(((methoxycarbonyl)-*D*-valyl-*D*-prolyl)oxy)acetyl)-[1,1'-biphenyl]-4-yl)-2-oxoethyl (methoxycarbonyl)-*L*-valyl-*L*-prolinate (**5**).

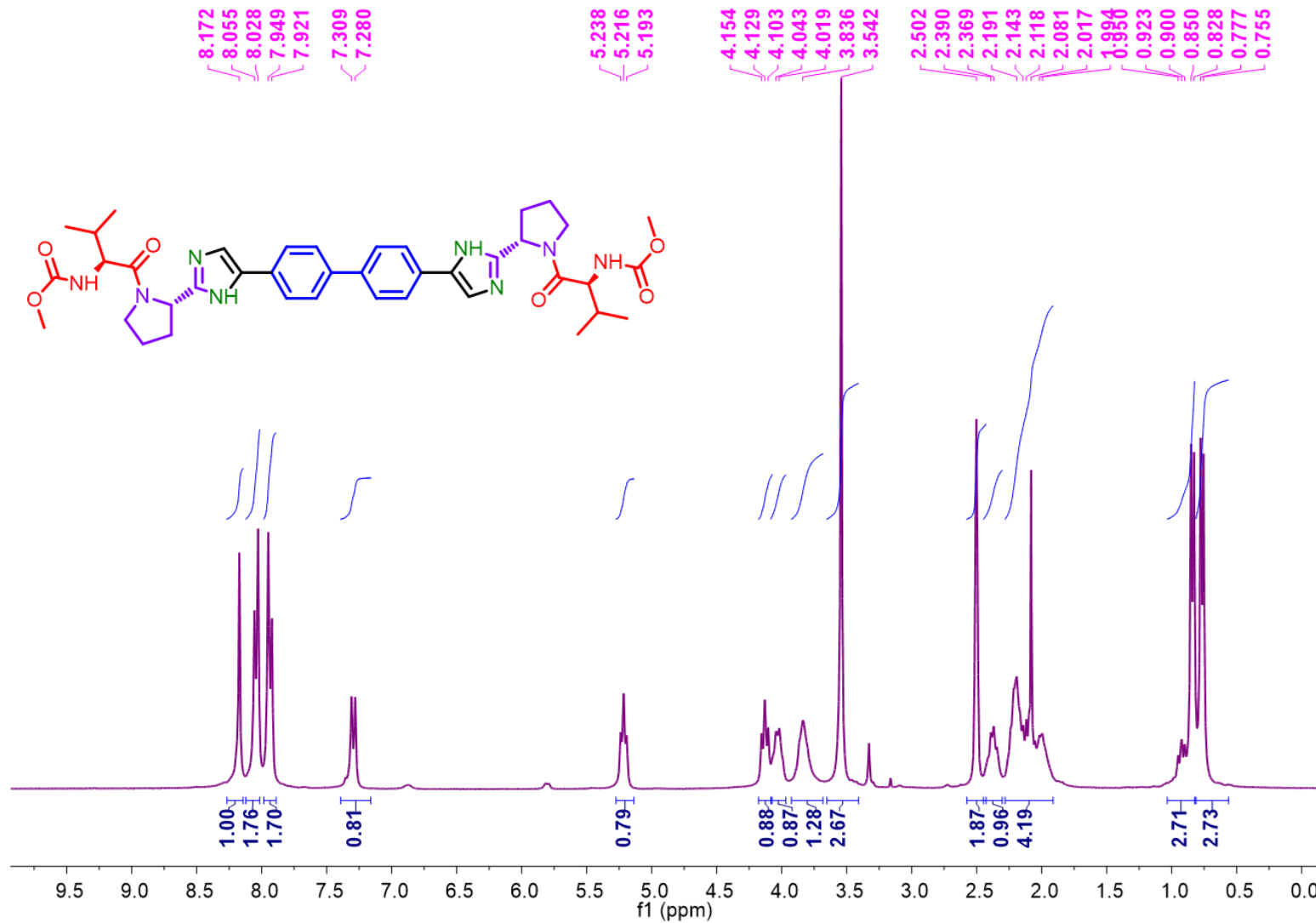


Fig. S37. ¹H NMR spectra of Daclatasvir (**6**) in DMSO-*d*₆.

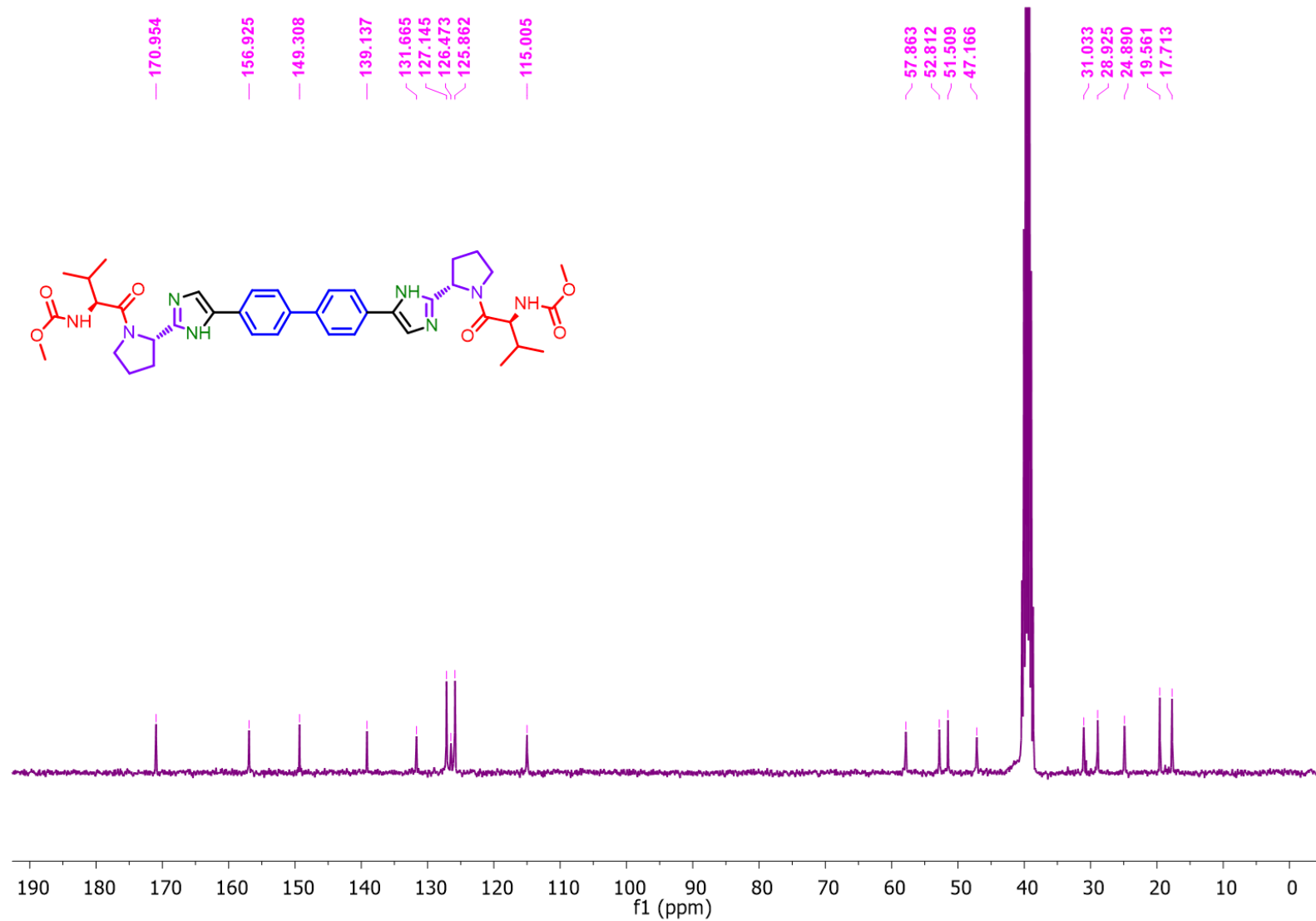


Fig. S38. ¹³C NMR spectra of daclatasvir (**6**) in DMSO-*d*₆.

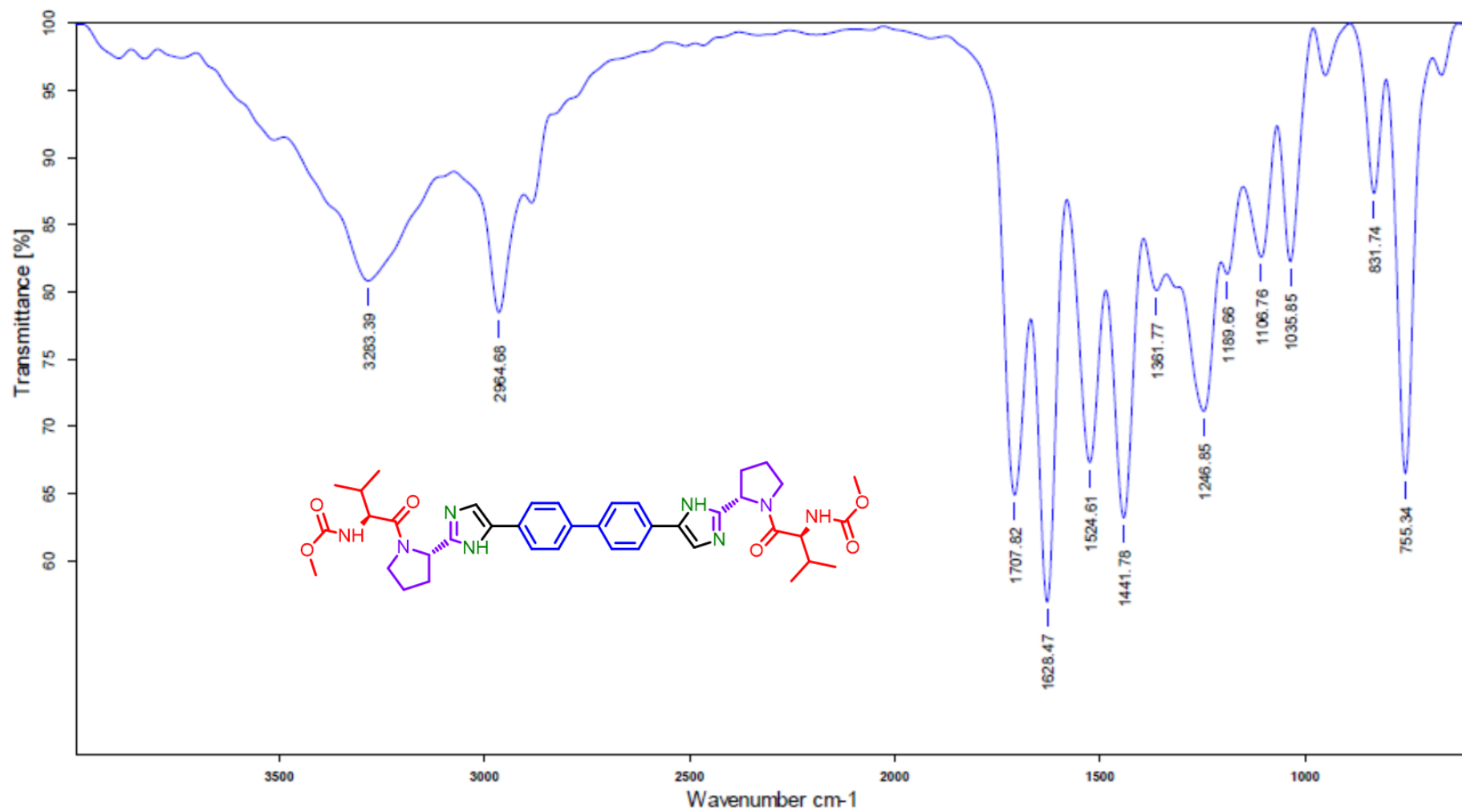


Fig. S39. IR spectra of daclatasvir (6).

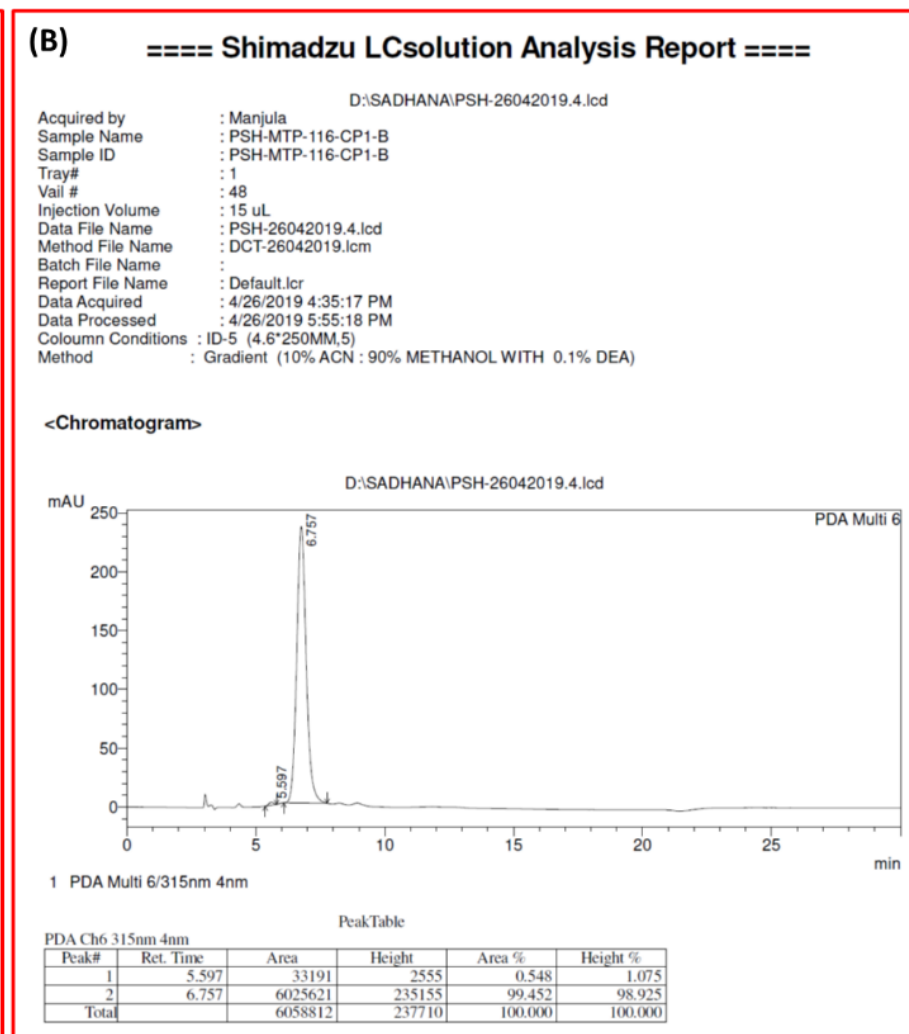
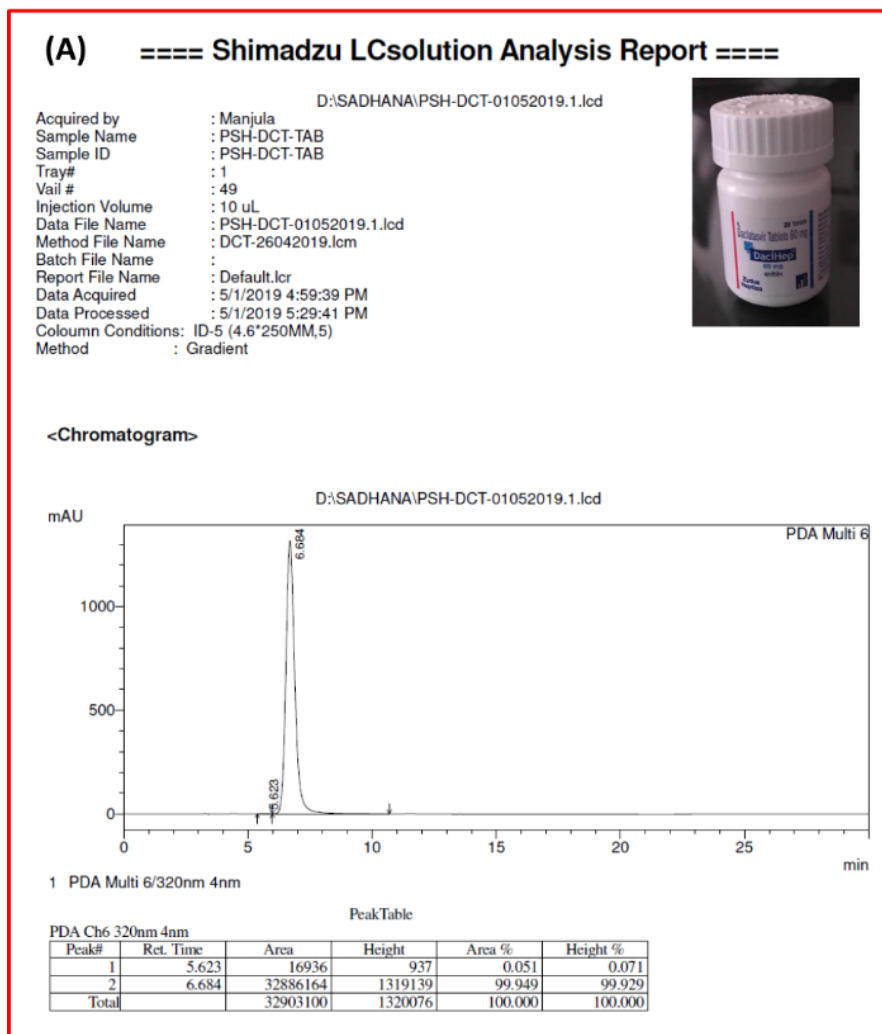


Fig. S40. Comparative HPLC data; (a) commercially available DCV; (B) Continuous flow-process synthesized DCV.

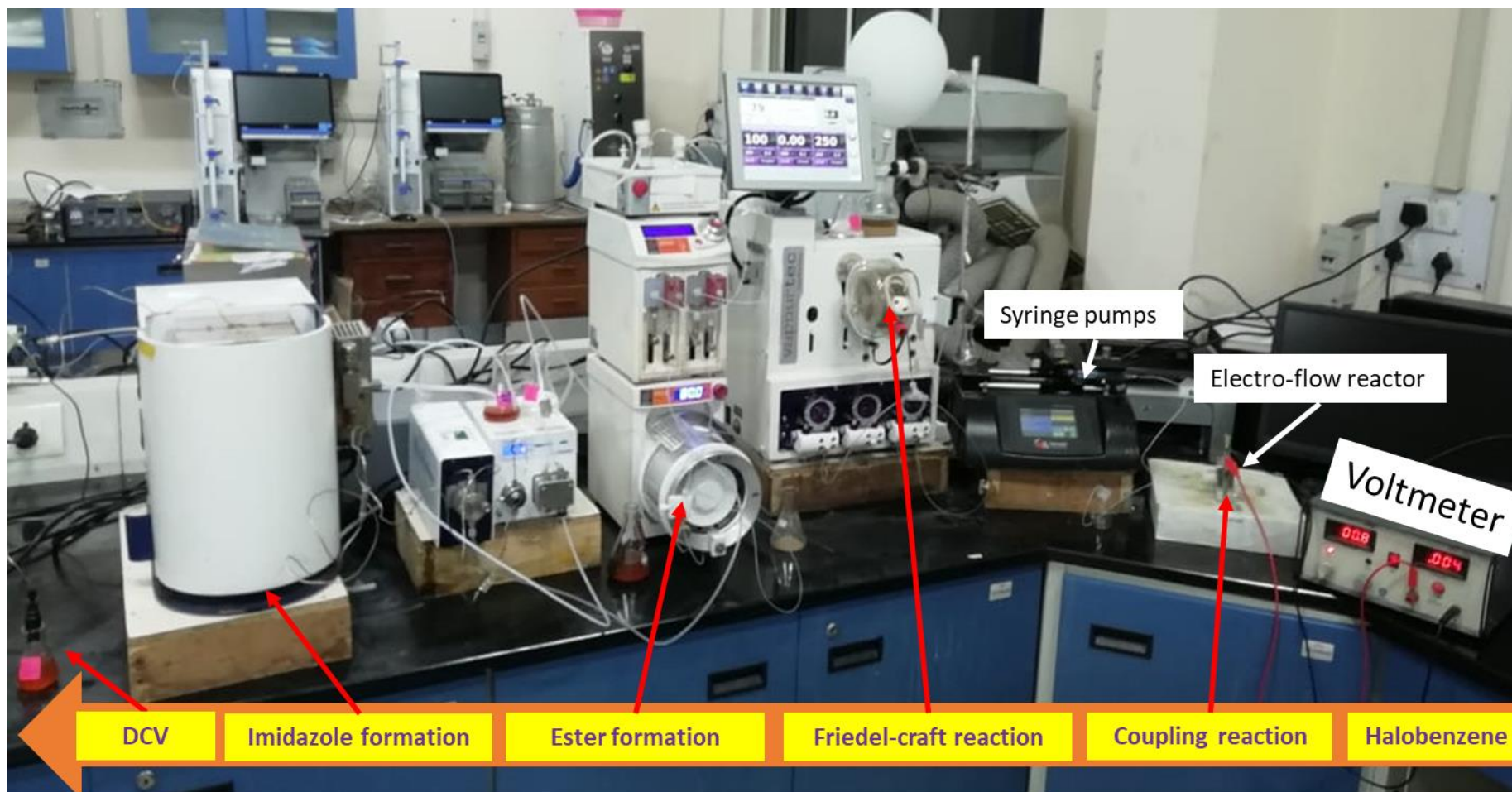


Fig. S41. Pictorial set-up for the halobenzene to DCV synthesis.

6. Supporting references

1. Ghosh, S. K.; Grover, A. K.; Dey, G. K.; Totlani, M. K. *Surf. Coat. Tech.* **2000**, *126*, 48.
2. Raub, M. E. B. C. J. *Platinum Metals Rev.* **1988**, *32*, 188.
3. Aand, D.; Karekar, S.; Mahajan, B.; Pawar, A. B.; Singh, A. K. *Green Chem.* **2018**, *20*, 4584.
4. Nadri, S.; Azadi, E.; Ataei, A.; Joshaghani, M.; Rafiee, E. *J. Organomet. Chem.* **2011**, *696*, 2966.
5. Li, J.-H.; Xie, Y.-X.; Yin, D.-L. *The Journal of Organic Chemistry* **2003**, *68*, 9867.
6. Pinxterhuis, E. B.; Visser, P.; Esser, I.; Gualtierotti, J.-B.; Feringa, B. L. *Angew. Chem. Int. Ed.* **2018**, *57*, 9452.
7. Buter, J.; Heijnen, D.; Vila, C.; Hornillos, V.; Otten, E.; Giannerini, M.; Minnaard, A. J.; Feringa, B. L. *Angew. Chem. Int. Ed.* **2016**, *55*, 3620.
8. Cheng, Y.; Gu, X.; Li, P. *Organic Lett.* **2013**, *15*, 2664.
9. Zhou, Y.; You, W.; Smith, K. B.; Brown, M. K. *Angew. Chem. Int. Ed.* **2014**, *53*, 3475.
10. Peng, Z.; Hu, G.; Qiao, H.; Xu, P.; Gao, Y.; Zhao, Y. *J. Org. Chem.* **2014**, *79*, 2733.
11. Vantourout, J. C.; Miras, H. N.; Isidro-Llobet, A.; Sproules, S.; Watson, A. J. B. *J. Am. Chem. Soc.* **2017**, *139*, 4769.
12. Johnson, J. J. L. D. S. *John Wiley & Sons*, **2015**, 43.
13. Medikonduri, S. S., Rammohan; Indukuri, Venkata Sunil Kumar; Kalindi, Srihari Raju; Chava, Satyanarayana *World Intellectual Prop. Org.* **2017**, *021904 A1*.
14. Seiwert, B. B. J. B. N. V. S. S. D. *WO2011075607A1* **2010**, *WO2011/075607*.
15. Hamm, S. K. P. P. G. M. J. S. J. *US Patent* **2008**, *US7728027B2*.